THE MECHANICAL AND ELECTRICAL PROPERTIES OF DIRECT-SPUN CARBON NANOTUBE MATS

J. C. Stallard*[1], W. Tan*, F. R. Smail*, T. S. Gspann†, A. M. Boies* and N. A. Fleck*.

*Department of Engineering, University of Cambridge, Trumpington Street, Cambridge, CB2 1PZ, UK.
†Department of Materials Science & Metallurgy, University of Cambridge, 27 Charles Babbage Road, Cambridge, CB3 0FS, UK.
[1] Corresponding Author: jcs202@cam.ac.uk

Abstract:

The mechanical and electrical properties of a direct-spun carbon nanotube mat are measured. The mat comprises an interlinked random network of nanotube bundles, with approximately 40 nanotubes in a bundle. A small degree of in-plane anisotropy is observed. The bundles occasionally branch, and the mesh topology resembles a 2D lattice of nodal connectivity slightly below 4. The macroscopic in-plane tensile response is elasto-plastic in nature, with significant orientation hardening. In-situ microscopy reveals that the nanotube bundles do not slide past each other at their junctions under macroscopic strain. A micromechanical model is developed to relate the macroscopic modulus and flow strength to the longitudinal shear response of the nanotube bundles. The mechanical and electrical properties of the mat are compared with those of other nanotube arrangements over a wide range of density.

Keywords: Carbon Nanotube Mat, Mechanical Properties, In-Situ Testing, Nanotube Bundles

1. Introduction

Individual carbon nanotubes (CNTs) possess exceptional mechanical and electrical properties [1]. The walls of CNTs have a Young's modulus of 1 TPa and a tensile strength of approximately 100 GPa [2], whilst isolated CNTs possess electrical conductivities of 2 x 10^7 s/m [3], ampacity of 10^{13} A/m^2 [4], and thermal conductivity of 3500 W/mK [5]. These properties are sufficiently impressive that significant research and industrial interest has arisen in the development of materials with CNTs as their primary constituents, and suitable for manufacture in industrial quantities. The *'Windle Process'* involves spinning a CNT aerogel from a gas phase, and has received much attention since the method was introduced by Li et al. [6] in 2004.

Methods for producing CNT materials may be divided into three families, together resulting in eight different types of CNT material. Figure 1 illustrates the three families, the methods which comprise them, and their morphologies. The first family involves processing vertically aligned CNTs grown from substrates by chemical vapour deposition; these CNT 'forests' may be (i) densified into pillars, (ii) spun into 1-dimensional fibres, or (iii) drawn into aligned 2-dimensional mats. The second family utilises liquids to create suspensions or solutions of short, mass-produced CNTs. CNT-solvent solutions can be filtered to create (iv) random planar 'buckypaper' mats, or spun into coagulating fluids to produce (v) single fibres. Porous CNT foams (vi) are

often produced from aqueous gel precursors by critical point drying, or freeze drying. The final family uses direct-spun carbon nanotube aerogels, produced via the 'Windle process'. Direct-spun fibres (vii) are produced by on-line solvent-condensation of the aerogels; alternatively, the spinning of aerogel layers onto a rotating mandrel, with or without solvent condensation, produces direct-spun mats, labelled (viii).

Charts that summarise the elastic moduli, strength, and electrical and thermal conductivity as a function of density for these CNT-based materials are presented in Figure 2. Note that the bulk density of CNT materials ranges from a few kg/m^3 for CNT foams to over 1000 kg/m^3 for CNT fibres, whilst their moduli range from tens of kPa to hundreds of GPa. Large differences in strength and conductivity are also observed. Wide property variations occur between classes and also within individual material classes. For example, direct-spun materials exhibit a large variation in mechanical properties due to their range of material alignment and density [7].

The macroscopic modulus of CNT materials is much below the Voigt upper bound, based on the in-plane modulus of a CNT wall (i.e. graphene). A similar observation can be made for strength as follows. If the ultimate tensile strength of CNT walls is assumed to be 100 GPa, all CNT morphologies lie more than an order of magnitude below the Voigt bound for ultimate tensile strength, as illustrated in Figure 2(b). In broad terms, the moduli and compressive yield strength of CNT foams and CNT forest based materials appear to scale with density ρ according to $E \sim \rho^3$ and $\sigma \sim \rho^2$ respectively. This scaling law is representative of cellular solids of low nodal connectivity [8].

The modulus and ultimate tensile strength of aligned CNT materials, such as fibres spun from solution and mats drawn from CNT arrays, vary by up to two orders of magnitude for a given density. Electrical conductivity also exhibits considerable variation between categories and also within individual categories. In the case of fibres spun from solution, a high electrical conductivity close to the Voigt bound is possible due to doping by acids, or by treatment with iodine [9]. The specific electrical conductivities of these materials are close to those of metallic alloys.

Now consider the chart of thermal conductivity versus density, see Figure 2(d). Aside from CNT foams, all categories of CNT materials have exceptionally high thermal conductivity compared to most other engineering solids. A line of specific thermal conductivity $\kappa/\rho = 0.0449$ m^4/Ks^3, equal to that of pure copper, has been added to Figure 2(d). This line lies well below that of many CNT materials.

Figure 3 presents a schematic of the continuous manufacturing method for direct-spun CNT materials as used in the present study, and the typical microstructure of CNT mat. A carbon source, often methane, is mixed with iron and sulphur catalysts and a carrier gas, typically hydrogen, in a furnace at 1570 K [10]. The catalysts initially vaporise but later, as the mixture cools, iron nanoparticles re-condense out of the gas phase. The iron particles grow, and develop a sulphur coating [11]. Fullerene caps form on the surface of the nanoparticles, and the nanoparticles then evolve into individual CNTs [12], and these in turn bind together into a network of CNT bundles by van-der-Waals attraction [11]. This network forms a cylindrical aerogel 'sock', and the sock is drawn from the reactor by winding it onto a mandrel. The degree of anisotropy in direct-spun CNT materials is sensitive to the ratio of draw speed to velocity of gas flow [7]. Many layers of drawn

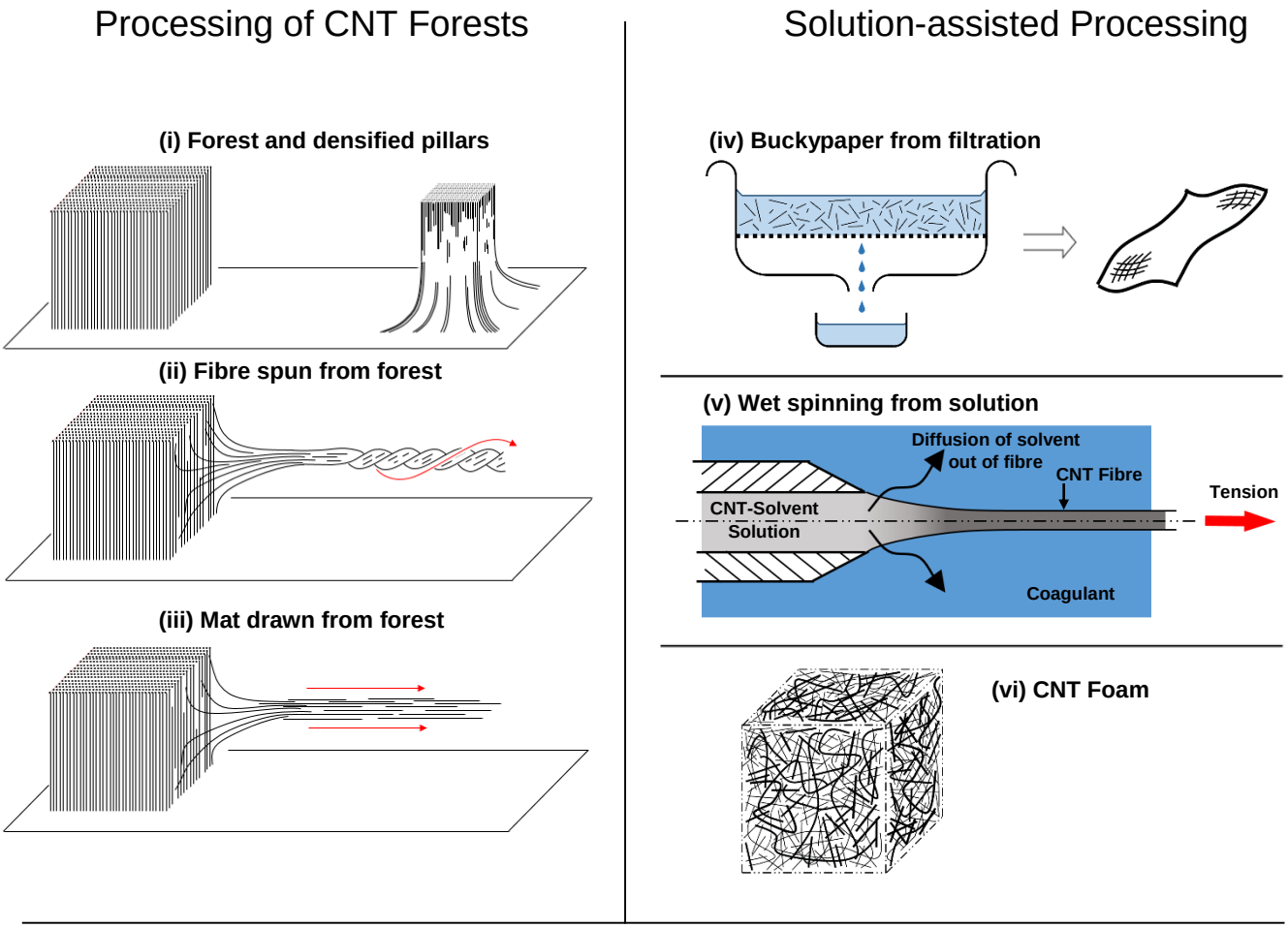

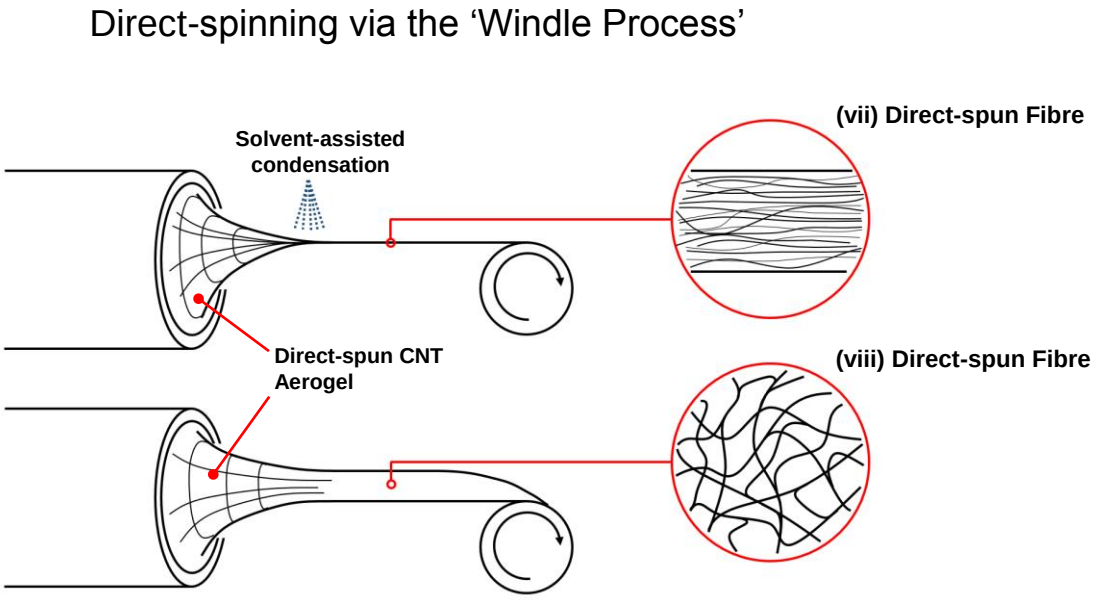

Figure 1: Classes of bulk CNT materials and production methods

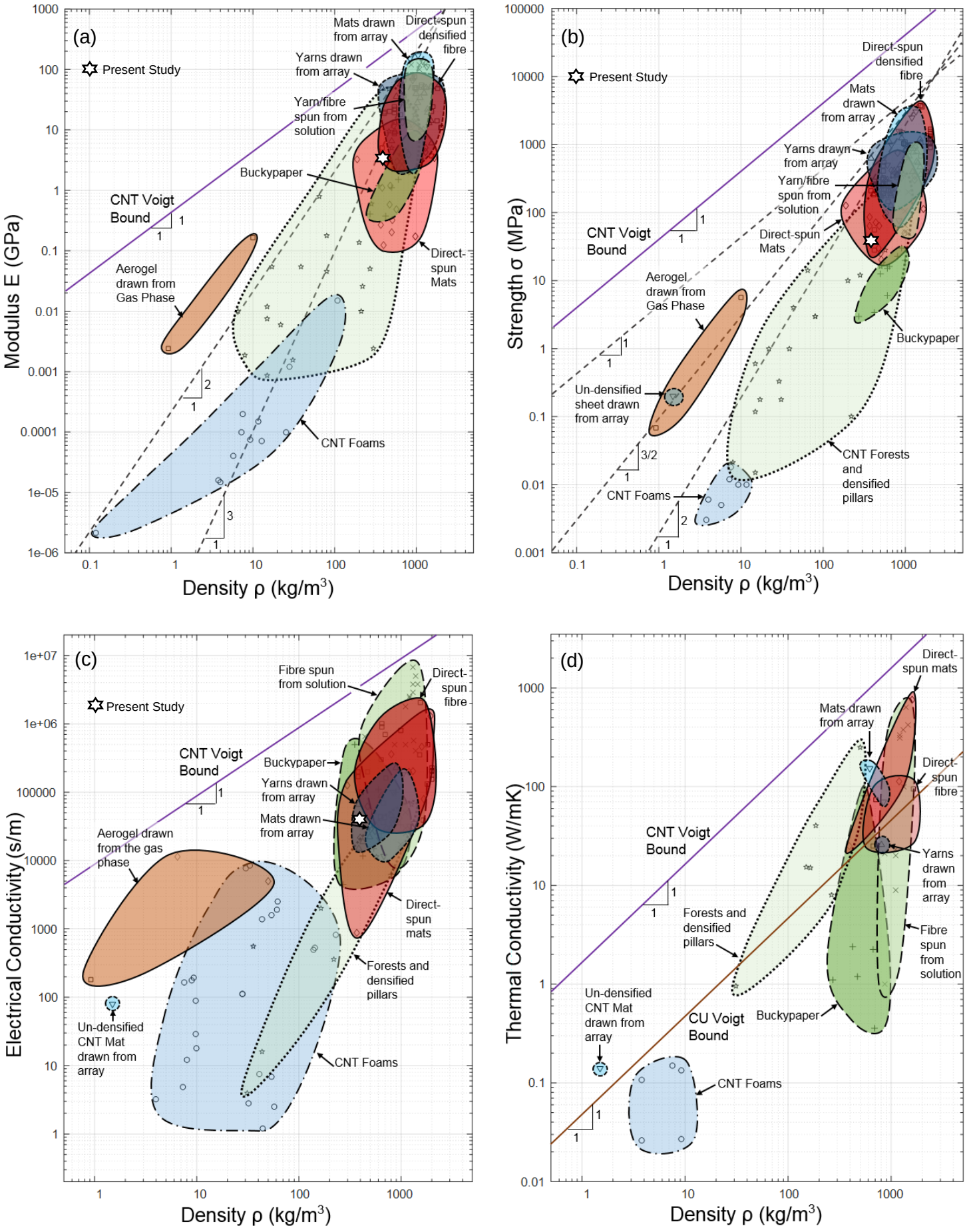

Figure 2: Material property charts and images of CNT materials: (a) modulus vs density, (b) strength vs density, (c) electrical conductivity vs density, (d) thermal conductivity vs density. References for the experimental data used in these property charts are included as supplementary material S1.

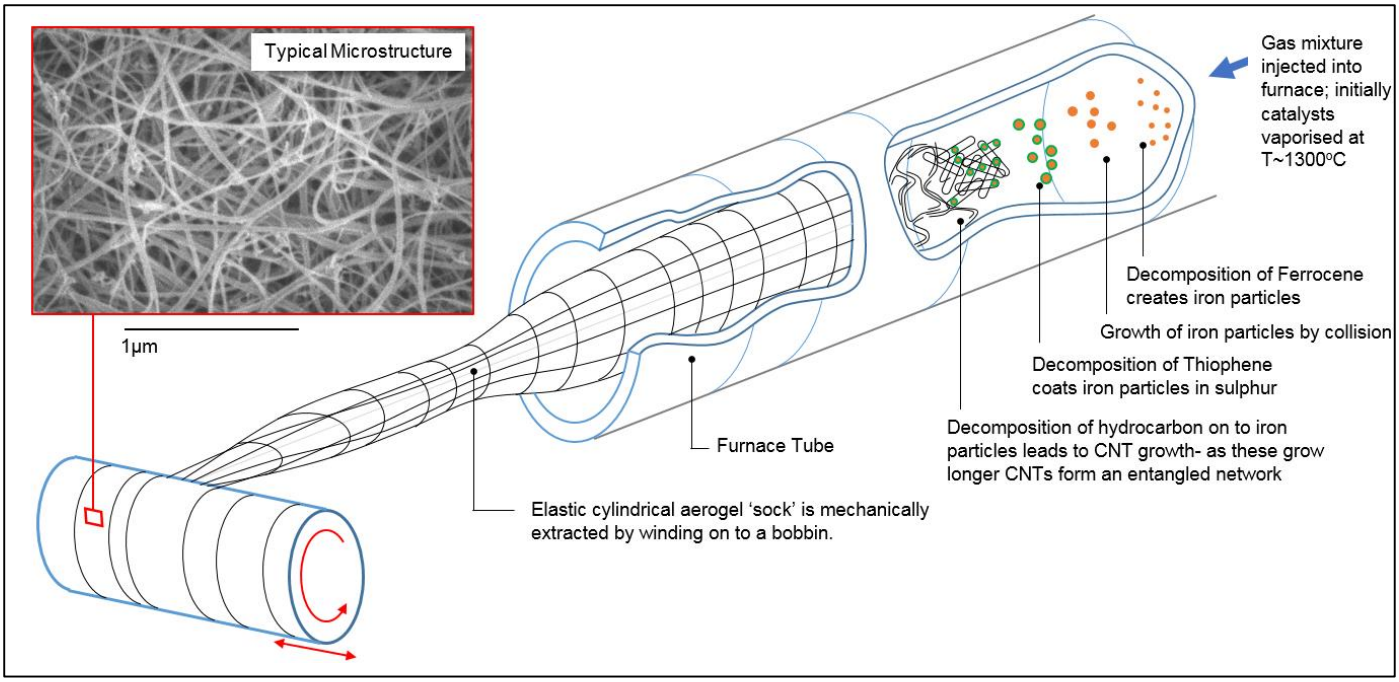

Figure 3: The 'Windle Process' for producing direct-spun CNT mat, and typical microstructure [6,7,10,11].

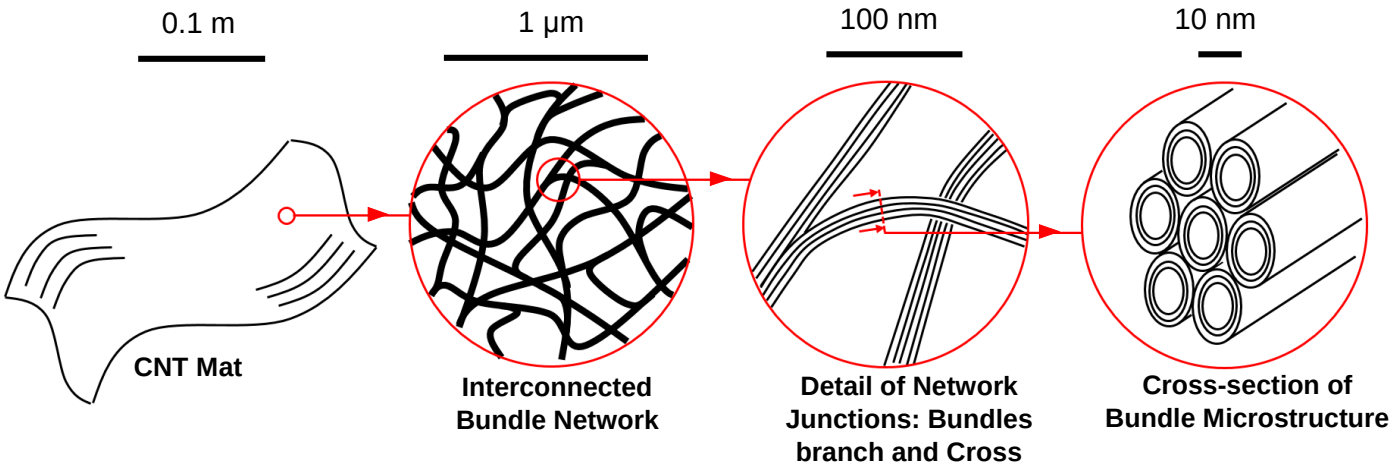

Figure 4: The hierarchical microstructure of direct-spun CNT mat.

CNT aerogel stack to form a carbon nanotube mat. Immersion in a solvent, typically acetone, followed by evaporation, results in capillary condensation and a thinner, denser sheet [13].

Direct-spun mats exhibit three distinct hierarchies of microstructure, as illustrated in Figure 4: the carbon nanotube, nanotube bundle, and the interlinked bundle network [14]. Although CNT bundles possess high tensile strength and stiffness in the axial direction [15], the weak van-der-Waals bonds between adjacent CNTs endow the bundles with a low longitudinal shear modulus and strength [16-18]. The interfacial shear strength between neighbouring CNTs within a bundle varies from 0.04 MPa to 70 MPa as a result of defects

within the walls [19,20], and the additional presence of a polymer coating inherent to the chemical vapour deposition process can raise the inter-bundle shear-strength to 400 MPa [21,22].

While microscopy studies of CNT mats during interrupted tensile tests [22-25] have shed light on microstructural changes in CNT mats due to strain, they do not inform us about the deformation mechanisms. To do so, in-situ observation is needed of microstructure evolution during tensile testing. In this study, we measure the nonlinear stress-strain response, piezoresistive behaviour [26] and electrical, physical and chemical properties of a commercially available direct-spun CNT mat. In-situ tensile tests reveal that the bundles undergo bending (and longitudinal shear) without slippage at junctions. A micromechanical model is then developed to relate the mechanical properties of the bundle network to those of individual bundles.

2. Materials and Methods

Direct-spun CNT mat was provided by Tortech Nano Fibers Ltd‡. Before characterisation, the mat was immersed in acetone for 5 minutes, dried in air for 20 minutes, and heated at 70 ˚C for 1 hour, to ensure that it was in the fully condensed state. The mat has a nominal thickness of 60 μm, as confirmed by optical interferometry and micrometre measurements. The areal mat density is 0.0234 kg/m^2, and the volumetric mat density is ρ_{Mat} = 390 kg/m^3. The chemical composition of the direct-spun mat was determined by thermogravimetric and Raman analysis, as described in Appendix A; the results revealed an Fe content of 6 wt. %, remainder CNT. A bundle density of ρ_B = 1560 kg/m^3 was determined by helium pycnometry; It follows immediately that the relative density of the mat is $\bar{\rho} = \rho_{Mat}/\rho_B$ = 0.25. Additional details of helium pycnometry are given in Appendix A.

Uniaxial tensile tests were performed using a screw-driven test machine, with the loading direction inclined at 0°, 45° and 90° to the draw direction of the CNT mat onto the mandrel. The test set-up is shown in Figure 5(a). The in-plane strain state was measured in the central portion of the sample by tracking the movement of dots of white paint applied prior to testing, using a digital camera and image processing software. Roller-grips enabled high tensile strains to be reached, with failure occurring at a strain level of 20% to 30%. In-situ tensile tests were conducted with a micro-test stage equipped with a 2N load cell, inside a scanning electron microscope (SEM).

The in-plane toughness G_c was measured by a trouser-tear test [27], illustrated in Figure 5(b). This toughness is determined from the steady state load for tearing, P_t, and the sample thickness, t_s, according to $G_c = 2\,P_t/t_s$ [28]. Trouser-tear tests were attempted in two directions, with the tear direction aligned with the draw direction, and in the transverse in-plane direction. Additionally, the out-of-plane delamination toughness, G_d, was quantified by a peel test [29], as illustrated in Figure 5(c). The toughness G_d is related to the peel force P_d and the sample width w_s according to $G_d = 2\,P_d/w_s$.

‡ Tortech Nano Fibers Ltd, Hanassi Herzog St., Koren Industrial park, Ma'alot Tarshiha, 24952 Israel.

Now consider the measurement of electrical properties. The in-plane and through-thickness electrical conductivity were measured using a 4-point probe method, as illustrated in Figure 6. A 4-point probe was also used to measure the in-plane electrical resistance during tensile testing, at a strain rate of $\dot{\epsilon} = 10^{-4}\,s^{-1}$. The tensile strain and in-plane resistance were measured with full, partial and cyclic unloading of stress, and a limited number of creep tests at constant stress were also performed.

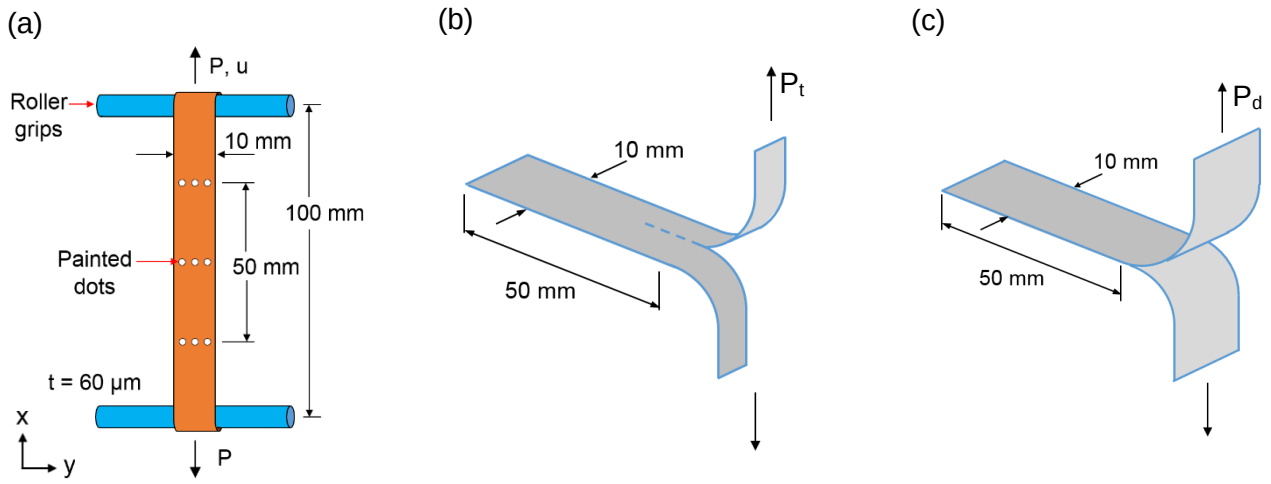

Figure 5: Mechanical testing techniques: (a) schematic of tensile test setup with sample dimensions and strain measurement techniques. (b) In-plane fracture 'trouser tear' test, (c) delamination peel test.

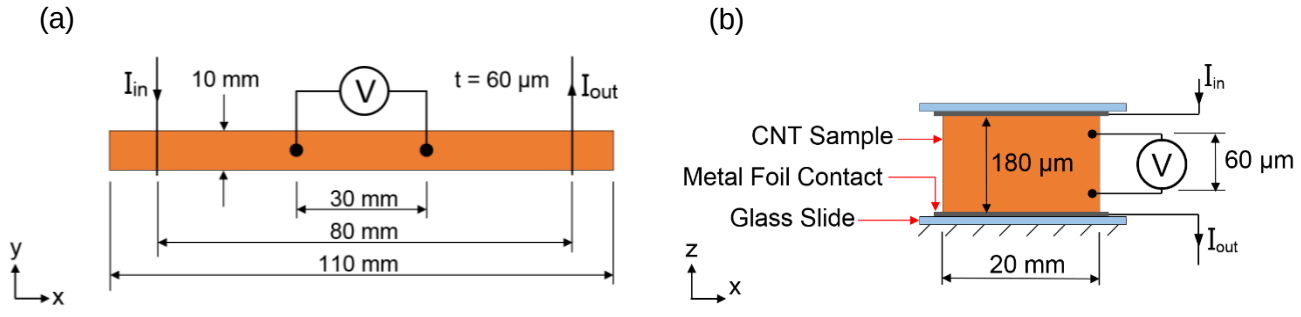

Figure 6: Four point probe measurement for (a) in-plane and (b) out of plane electrical conductivity.

3. Results

a. Uniaxial Tensile Response

The nominal stress-strain response, as illustrated in Figure 7(a), exhibited an initial linear behaviour, followed by a strain-hardening plastic response at approximately 4% strain. Above 15% strain, the hardening rate increases. The response has a moderate degree of anisotropy. The in-plane transverse strain is plotted as a function of tensile strain in Figure 7(b). The apparent Poisson's ratio, ν_{12}, initially equals 0.6, but increases to between 2.7 and 3.5 at higher strains. An explanation for these high values of ν_{12} is evident from images taken during in-situ tensile testing, see Figure 7(c), which illustrates the appearance of out-of-plane wrinkles at the micron level. This wrinkling appears to contribute to the compressive transverse strain. No noticeable rate dependency was observed for strain rates between 10^{-4} s^{-1} and 10^{-2} s^{-1}, as illustrated in Figure 7(d) for samples aligned with the draw direction.

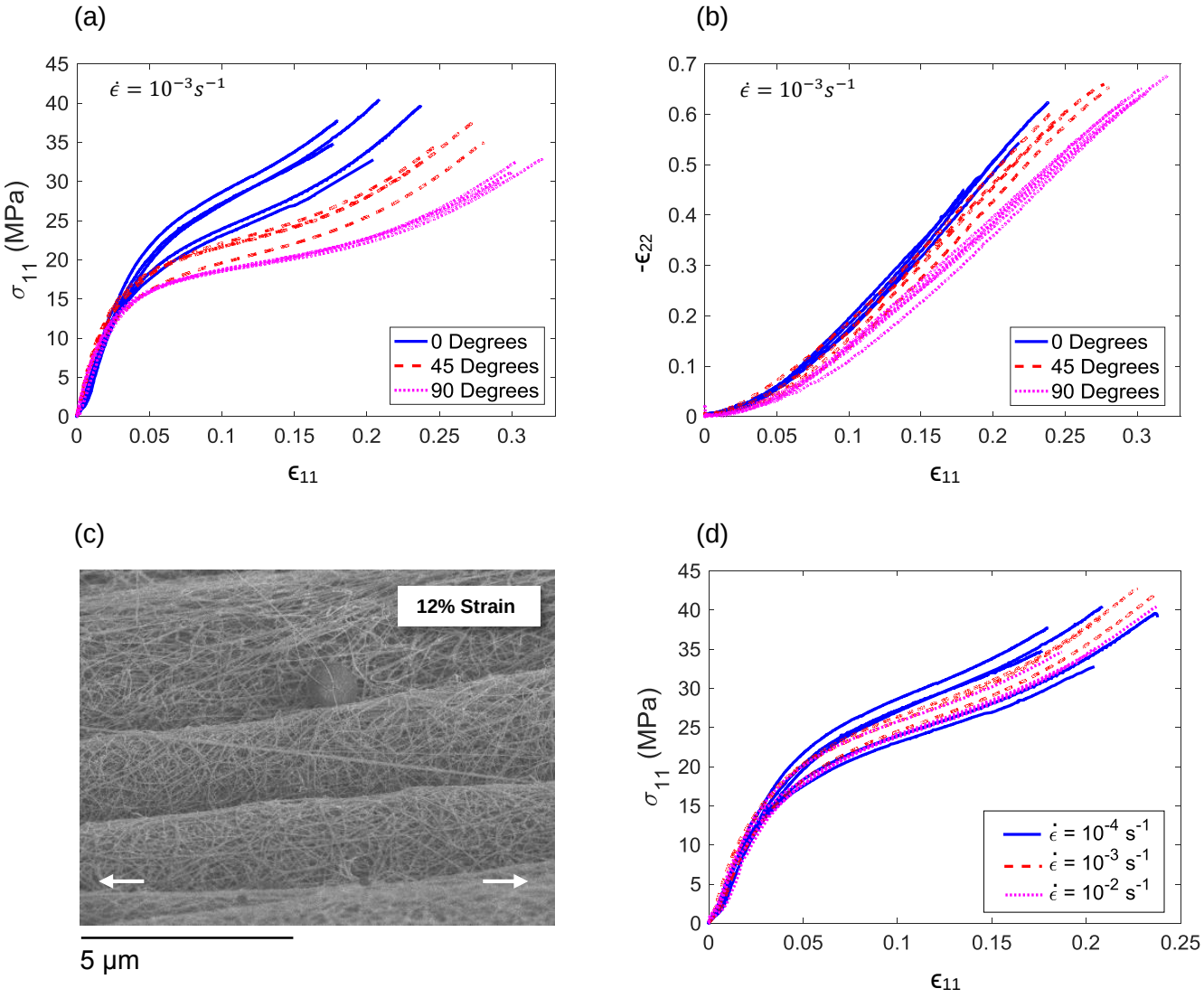

Figure 7: Uniaxial tensile response: (a) in-plane stress-strain response for different material orientations, (b) relationship between tensile and transverse strains. (c) illustrates the appearance of transverse wrinkles during in-situ tensile testing; the arrows indicate the direction of tensile straining. (d) records the effect of strain rate on the uniaxial tensile response for samples aligned with the draw-direction.

b. Toughness

Trouser-tear tests along the draw direction were performed from starter cracks cut parallel to the draw direction. The average value of tear energy from these trouser tests was $G_c = 22$ kJ/m^2. Trouser-tests were unable to grow cracks transverse to the draw direction; instead, kinking of the starter crack occurred and no useful data were obtained. The delamination toughness from a peel test was found to be $G_d = 5.4$ J/m^2. This is about four orders of magnitude below the in-plane toughness.

c. Electrical Properties

The in-plane conductivity exhibited a small degree of anisotropy, with values of 404 s/cm parallel to the manufacturing draw direction, 358 s/cm at 45º, and 325 s/cm at 90°. In the through-thickness direction, electrical conductivity was about 6 orders of magnitude lower, at 6.39x10^{-4} s/cm.

d. Unloading Response and Creep Tests

A 4-point probe, as illustrated in Figure 8(a), was used to measure the in-plane electrical resistance during tensile testing, at a strain rate of $\dot{\epsilon}$ = 10^{-4} s^{-1}. The tensile strain and in-plane resistance were measured with full, partial and cyclic unloading of stress, and also at constant stress. Typical responses are presented, with sample resistance normalised by the initial resistance R_0.

The stress-strain and resistance-strain response with periodic partial unloading of samples at 0˚, 45˚ and 90˚ to the draw direction are illustrated in Figure 8(b). Despite the presence of structural anisotropy, the piezoresistive response, R/R_0 versus ϵ_{11}, is qualitatively similar for all directions. Little mechanical or electrical hysteresis is present upon partial unloading. We define the unloading stiffness E_U during the unloading cycle as $E_U = \Delta\sigma_{11}/\Delta\varepsilon_{11}$, where $\Delta\sigma_{11}$ is the change in nominal stress during unloading and $\Delta\varepsilon_{11}$ is the corresponding change in true strain. The gauge factor, GF, is defined as $GF = \Delta(R/R_0)/\Delta\varepsilon_{11}$, where $\Delta(R/R_0)$ is the change in normalised sample resistance during the unloading cycle. The unloading stiffness and gauge factor are plotted against nominal strain in Figure 8(c). E_U increases with strain for all sample orientations, with the initial rate of increase highest for the 0˚ samples. The gauge factor during unloading also increases with strain.

Figure 8(d) illustrates the effect of full unloading for a sample oriented at 0° to the draw direction. Both the resistance-strain and stress-strain responses exhibit hysteresis, and both a permanent strain and permanent change in sample resistance are evident upon unloading.

A stable response to cyclic stress is of importance in many sensing and structural applications. An initial exploration into the response under cyclic uniaxial loading was conducted by applying four loading packets of ten unloading cycles, with results as illustrated in Figure 8(e). The loading packets labelled 1, 2, and 3 all resulted in permanent drift in the piezoresistive and stress-strain responses. The last set of loading cycles involved cyclic excursions well below the current yield strength, as denoted by the symbol $\Delta\sigma$ in Figure 8(e). This loading packet gave rise to an elastic response.

The creep behaviour of the CNT mat was investigated by holding a sample at a constant tensile stress of 8.3 MPa, 17 MPa, and then at 25 MPa, each time for 1500 seconds, before unloading the sample to 17 MPa for a further 1500 seconds. The strain, ϵ_{11}, recorded at each of these constant stresses is plotted against time in Figure 8(f). No noticeable creep was observed in the final phase of holding at 17 MPa. Also, no noticeable change in electrical resistance occurred whilst the sample was held at constant stress.

e. In-Situ Observations of Deformation Mechanisms

An understanding of the origin of mechanical properties in direct-spun mats is aided by observation of the deformation mechanisms at the microstructural scale. Unlike other in-situ studies of CNT mats that have been reported in the literature [24,25], in the present study the same microstructural area is observed before and after deformation. This enables us to identify the main mechanisms of deformation. For example, images of microstructure are presented in Figures 9(a) and (b), for strains of $\epsilon = 0\%$, and 10% respectively, with specific bundles and locations of interest annotated. The bundles labelled 1 and 2 straighten and orient along the loading direction, whereas the transverse bundle labelled 3 undergoes buckling.

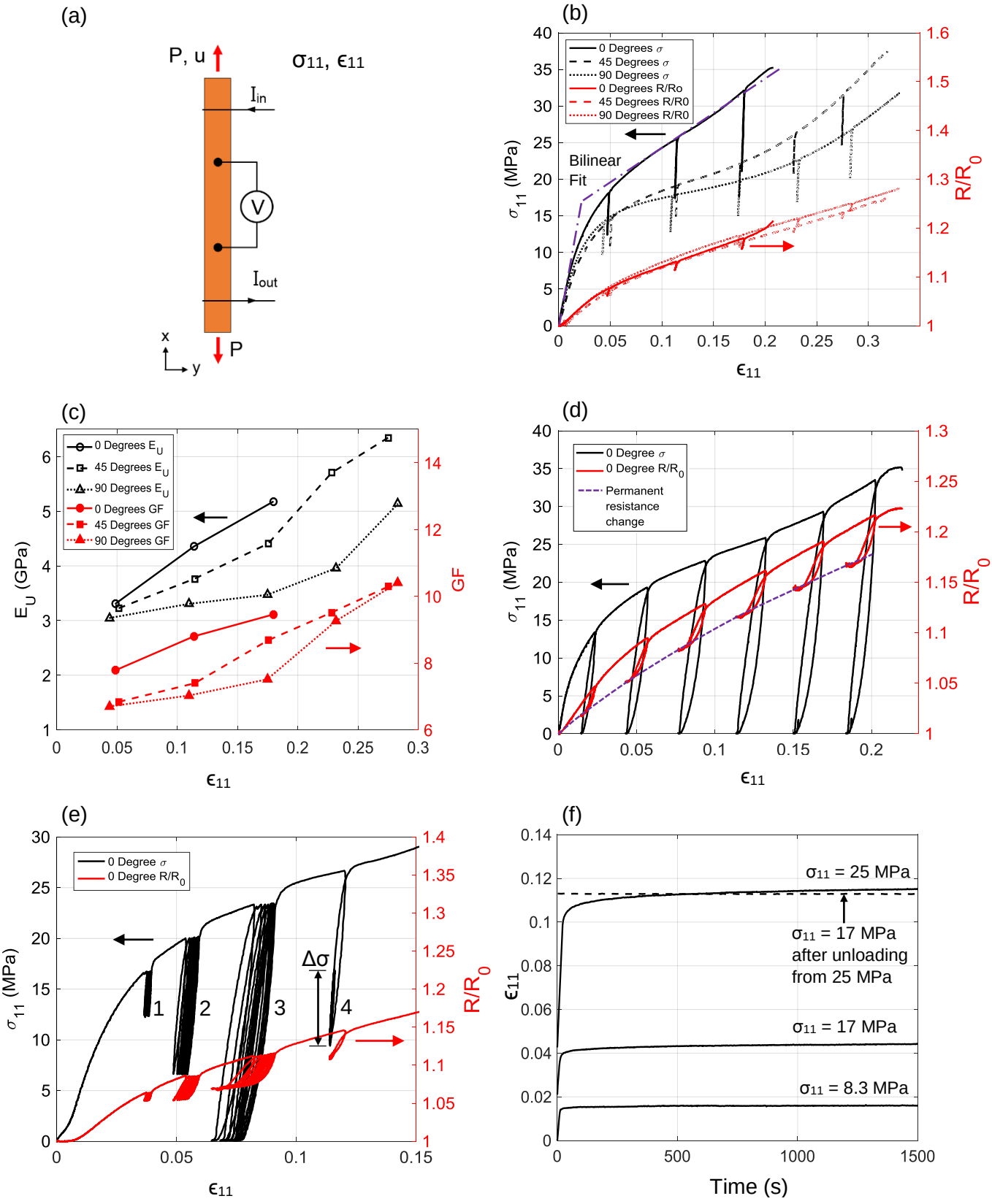

Figure 8: Nonlinear and piezoresistive behaviour of carbon nanotube mat: (a) schematic of tenslie test setup with four proint probe, (b) anisotropic response with partial unloading, (c) unload modulus and gauge factor as a function of applied strain for different sample orientations to the draw-direction, (d) full unloading cycles revealing permanent strains and resistance change, (e) drift and hysteresis when cycling up to the yield surface, and (f) creep curves showing the effects of constant stress on the tensile strain. Unless otherwise stated, stresses and strains are nominal, as calculated from initial sample dimensions.

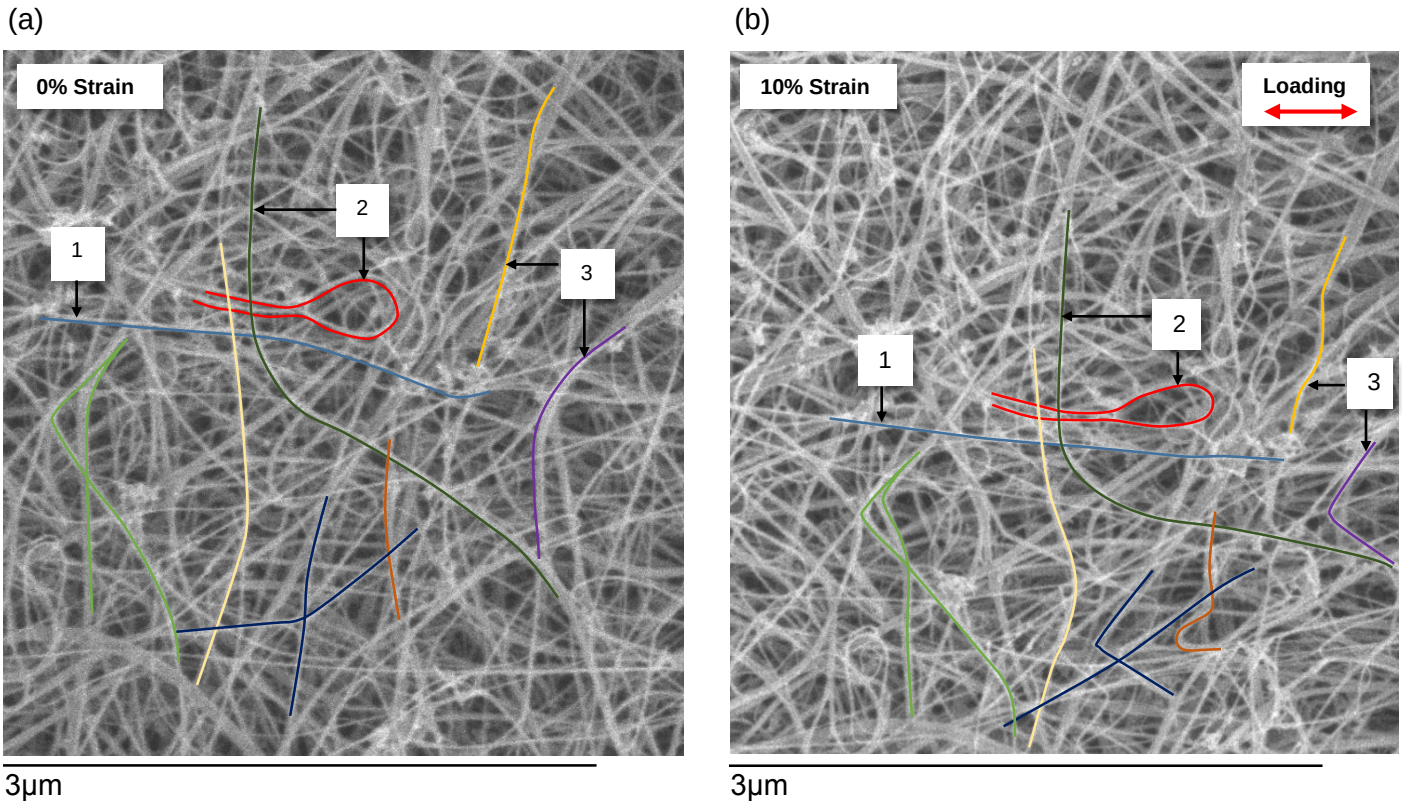

Figure 9: Microstructural changes during yield: (a) shows a piece of CNT mat microstructure prior to loading, and (b) at 10% macroscopic strain, with bundles and areas of interest highlighted for discussion.

4. A Model for in-plane Mechanical Properties

There is a major deficit in stiffness and strength when one compares individual CNTs with bulk CNT materials. In the case of direct-spun mats, why does a random, interconnected network of CNT bundles possess inferior tensile properties to those of individual CNTs? This question is addressed via the model below.

At the microstructural level, the junctions between CNT bundles are of low nodal connectivity, of between 3 and 4. Consequently, the mechanical properties are governed by the bending and shear response of CNT bundles, rather than by axial stretch [30]. For an approximate prediction of stiffness and strength, this justifies the use of a periodic 2D honeycomb unit cell, as illustrated in Figure 10(a), with struts of thickness t and length l that deform by bending and shearing [8,30]. CNT bundles form the struts of this unit cell, and are connected to one another at nodes by the exchange of nanotubes from one bundle to the next. We write the relative density of the network $\bar{\rho} = \rho_{Mat}/\rho_B$ as [8]:

$$\bar{\rho} = \frac{3}{2\cos\omega\,(1+\sin\omega)}\left(\frac{t}{l}\right), \tag{1}$$

where ω is the angle of the inclined strut to the horizontal, see Figure 10(a). For a regular honeycomb, ω equals $\pi/6$. Upon neglecting axial stretch of the struts, and upon taking P as the load on each vertical strut, we analyse one half of a beam inclined to the loading direction using Timoshenko beam theory, and apply

symmetry boundary conditions, as illustrated in Figure 10(b). The beam of length $l/2$ is built-in at its left-hand end, labelled $L1$, and is subjected to an end load $P/2$ at its point of inflection $(M = 0)$, at location $L2$. The co-ordinate along the beam mid-surface is x. The bending moment along the beam $M(x)$ and shear force $Q(x)$ are given by:

$$M(x) = \frac{P}{2}\left(\frac{l}{2} - x\right)\cos\omega\,, \tag{2}$$

and

$$Q(x) = \frac{P}{2}\cos\omega\,, \tag{3}$$

respectively. Now, write ϕ as the angle of rotation of the normal to the mid-surface and w as the transverse displacement of the mid-surface. Then, Timoshenko beam theory [31] for a bundle of axial Young's modulus E_B and shear modulus G_B states that:

$$M(x) = E_B I\frac{\partial\phi}{\partial x}\,, \tag{4}$$

and

$$Q(x) = sAG_B\left(-\phi + \frac{\partial w}{\partial x}\right), \tag{5}$$

where I is the second moment of area, A the cross-sectional area, and the shear coefficient equals $s = 8/9$ [31]. We substitute equation (4) into (2) and integrate to obtain

$$\phi = \frac{x(l-x)\cdot P\cos\omega}{4E_B I}\,. \tag{6}$$

Substitution of equation (6) and (3) into (5), followed by rearrangement and integration, yields

$$w = \frac{Px\cos\omega}{2sAG_B} + \frac{\left(\frac{x^2 l}{2} - \frac{x^3}{3}\right)\cdot P\cos\omega}{4E_B I}\,. \tag{7}$$

Since $\delta = w\left(x = \frac{l}{2}\right)$, we find that

$$\delta = \left(\frac{l}{4sAG_B} + \frac{l^3}{48E_B I}\right)P\cos\omega\,, \tag{8}$$

and the macroscopic strain ϵ^∞ in the direction of loading follows immediately as

$$\epsilon^\infty = \frac{2\,\delta\cos\omega}{(1+\sin\omega)l}\,. \tag{9}$$

Now, the macroscopic stress σ^∞ is given by $\sigma^\infty = P/(2lb\cos\omega)$, and upon making the substitution for the bundle area $A = tb$, and the second moment of area $I = bt^3/12$, the macroscopic modulus $E_{Mat} = \sigma^\infty/\epsilon^\infty$ reads

$$E_{Mat} = \frac{1+\sin\omega}{\cos^3\omega}\left[\frac{1}{sG_B}\left(\frac{l}{t}\right) + \frac{1}{E_B}\left(\frac{l}{t}\right)^3\right]^{-1}. \quad (10)$$

It remains to estimate the shear modulus G_B and axial modulus E_B for a bundle. Whilst the axial bundle modulus derives from covalent bonding within the CNT wall, the shear modulus is dictated by the much more compliant van-der-Waals bonding between adjacent CNTs. We follow the approach of [18] in estimating the axial bundle modulus as $E_B = (\rho_B/\rho_w)E_w$ where $\rho_w = 2200$ kg/m^3 (i.e. that of graphene at an interlayer spacing of 0.34 nm). For $E_w = 1$ TPa, it follows that $E_B = 680$ GPa. Values for G_B in literature have been deduced from in-situ 3-point bending tests [16,17], and from thermal vibration [32], varying from 0.7 to 6.5 GPa $\pm$ 50%. Our measured mat modulus of 3.3 GPa from unloading tests and assumed value for E_B implies $G_B = 9.5$ GPa via equation (10), which is within the range of experimental measurements [16]. Inspection of equation (10) reveals the relative contribution of the shear and bending deformation to the macroscopic modulus. Since $sG_B \ll E_B(t/l)^2$, it is clear that the shear modulus of the CNT bundle dominates the deformation, as opposed to the stiffer covalent bonding along the CNT walls.

Now consider the tensile yield strength of the hexagonal lattice. The tensile stress on the outermost fibre of the inclined strut, due to the bending moment $M(x)$ and axial tension, is given by $\sigma_B = Mt/2I + (P/2tb)\sin\omega$, whereas the average shear stress on the cross section due to the shear force $Q(x)$ is given by $\tau_B = Q(x)/A$. As the bending moment is greatest at the location labelled $L1$ on the inclined strut illustrated in Figure 10(b), σ_B and τ_B have the following maximum values:

$$\sigma_B = \left(\frac{27}{4(1+\sin\omega)^2\bar{\rho}^2} + \frac{3\sin\omega}{2(1+\sin\omega)\,\bar{\rho}}\right)\sigma^\infty \quad , \quad (11)$$

and

$$\tau_B = \left(\frac{3\cos\omega}{2(1+\sin\omega)\bar{\rho}}\right)\sigma^\infty \quad . \quad (12)$$

The ratio between bundle tensile stress and average shear stress is given by

$$\frac{\sigma_B}{\tau_B} = \frac{9}{2\cos\omega\,(1+\sin\omega)\bar{\rho}} + \frac{\sin\omega}{\cos\omega} \quad . \quad (13)$$

Now, for a relative density $\bar{\rho} = 0.25$ and $\omega = \pi/6$, it follows that $\sigma_B/\tau_B = 14.4$. If the ratio of bundle tensile strength σ_{Bf} to bundle shear strength τ_{bf} is greater than σ_B/τ_B, macroscopic yield will be limited by the bundle shear strength, rather than by the fracture of CNT walls. We argue that this is the case, on the basis that that the ratio σ_{Bf}/τ_{Bf} is more than four times greater than σ_B/τ_B, with the following justification.

Tensile tests conducted on individual CNT bundles grown by the chemical vapour deposition process suggest that the wall fracture strength of individual CNTs σ_{wf} lies between 5.5 GPa and 25 GPa [22]. Assume that the bundle strength scales with the CNT wall strength σ_{wf} according to $\sigma_{Bf} = (\rho_B/\rho_w)\sigma_{wf}$, and take $\sigma_{wf} =$ 5.5 GPa. Then, the bundle fracture strength equals $\sigma_B = 3.7$ GPa.

Now consider the CNT bundle shear strength τ_{Bf}. Values for the bond shear strength between CVD-grown tubes, as measured in the literature, vary from 0.04 MPa to 70 MPa [19,20], with values sensitive to the concentration of graphitic defects [20,33]. For adjacent pristine CNT surfaces with long overlap lengths, the bond shear strength lies between 30 MPa and 60 MPa [34]. Here, we shall assume the value $\tau_{Bf} = 60$ MPa, as this implies a macroscopic yield stress of 17 MPa from equation (12), close to our experimental measurements, and lies within the range of values reported in literature. Consequently, $\sigma_{Bf}/\tau_{Bf} = 62$, and we conclude that the macroscopic yield strength is limited by the bundle shear strength.

Our conclusion that the shear strength of CNT bundles limits the macroscopic yield strength of direct-spun mats, as opposed to the bundle axial strength, is consistent with our observations of bundle deformation during in-situ testing, and explains why the random arrangement of CNT bundles within the mat results in a severe knockdown in mechanical properties when compared to those of individual CNTs in longitudinal tension.

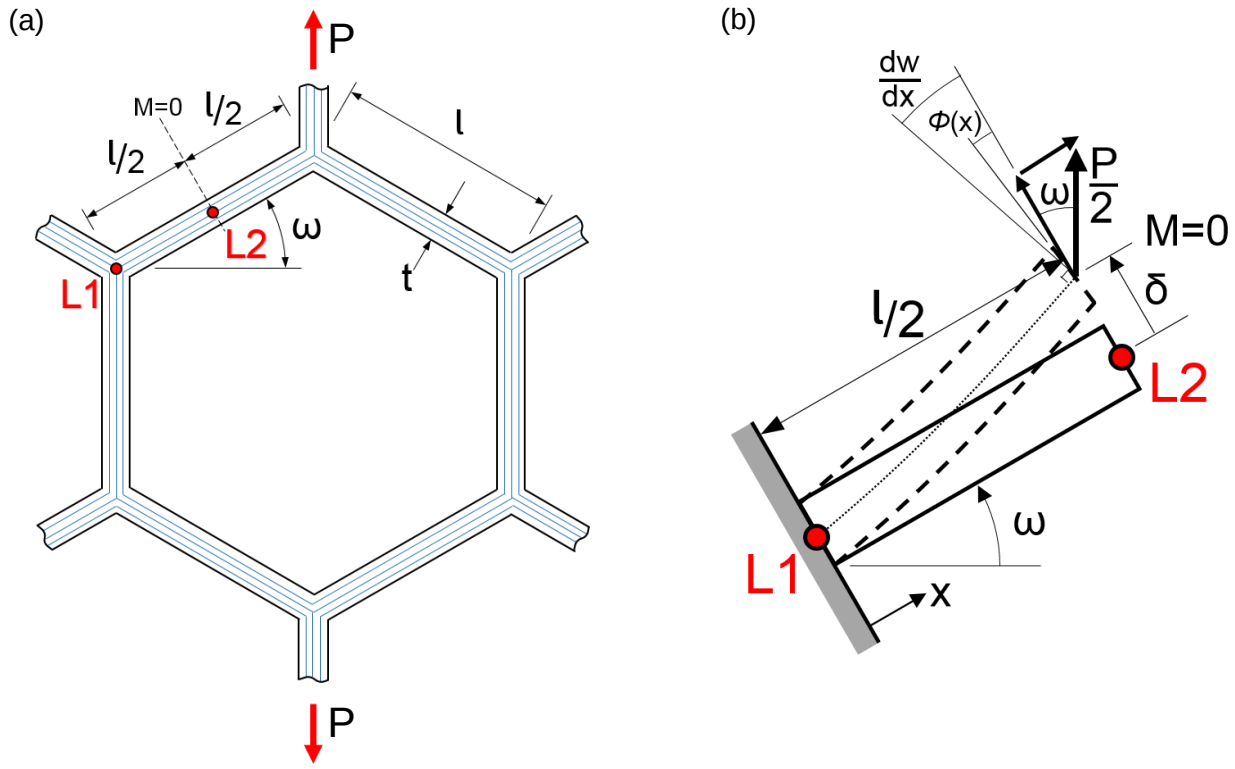

Figure 10: (a) Geometry of a honeycomb unit cell of CNT bundle network microstructure (depth b into page), (b) loading and deformation of an inclined strut modelled with Timoshenko beam theory.

5. Conclusions

The mechanical, electrical and thermal properties of direct-spun mats, fibres, and other CNT materials were compared over a wide range of densities. Characterisation of a commercially produced direct-spun mat revealed in-plane electrical conductivities of between 325 s/cm and 404 s/cm, elastic moduli of 3.0 GPa to 3.4 GPa, and an ultimate tensile strength between 30 MPa and 40 MPa. The through-thickness electrical conductivity and the mechanical properties of the bond between adjacent layers within the CNT mat were found to be much less than in-plane properties. Macroscopic deformation of CNT mat is accompanied by reorientation of the bundle network along the loading direction. A micromechanical model was developed to relate macroscopic direct-spun mat properties to those of CNT bundle network. It illustrates that the longitudinal shear deformation of CNT bundles dominates, and accounts for the knockdowns in CNT mat mechanical properties compared to those of an individual CNT in uniaxial tension.

Acknowledgements: *The authors acknowledge the assistance of Simon Griggs of the Department of Materials Science for assistance with in-situ microscopy, Hadi Modarres and Michael De Volder of the Institute for Manufacturing for assistance with Thermogravimetric Analysis, and Tortech Nano Fibers Ltd. for supplying CNT mat. The authors acknowledge funding from the EPSRC project 'Advanced Nanotube Application and Manufacturing (ANAM) Initiative' under Grant No. EP/M015211/1.*

Conflict of Interest: *The authors have no conflicts of interest to declare.*

Appendix A: Composition of the Direct-Spun Mat

The chemical composition of the mat was determined by thermogravimetric analysis, conducted using a PerkinElmer TGA 4000. The temperature was held at 100 °C to remove adsorbed moisture, then increased at a scan rate of 5 °C/min. The results revealed an Fe content of 6 wt. %, remainder CNT; the relationship between sample mass and temperature, and the rate of mass change with respect to temperature are plotted in Figure A.1(a).

The Raman spectrum of the CNT mat was obtained with an EZRAMAN-N instrument, using a laser power of 50 mW, and 3 scans at 30 seconds integration time. A Raman spectrum of the CNT mat is illustrated in Figure A.1(b). The high intensity G-band at 158 mm^{-1} corresponds to vibration of sp^2 bonds. Dividing the G-band intensity by that of the D-band at 134 mm^{-1} gives a G/D ratio of 4.5. The D-band results from the breathing mode of a six-fold aromatic ring, and cannot occur unless disorder is present, either in the crystalline structure of the CNT walls, or in the form of additional amorphous carbon materials [35,36]. The relatively high G/D ratio observed here indicates that neither of those defects are particularly prevalent. The absence of radial breathing modes at low frequency (<50 mm^{-1}) indicates that small diameter single- or double-walled CNTs are not present within the mat [35].

Bundle density was determined with helium pycnometry (performed by Quantachrome UK Ltd). This involves placing a CNT mat sample in a chamber of known volume, which is then purged of air and pressurised with helium gas. After the pressure of this chamber is measured, a valve is opened to link it with another chamber of known volume, initially at vacuum. After the pressure has stabilised, it is recorded; the perfect gas law is then used to calculate the sample volume from the measured gas pressures and known chamber volumes.

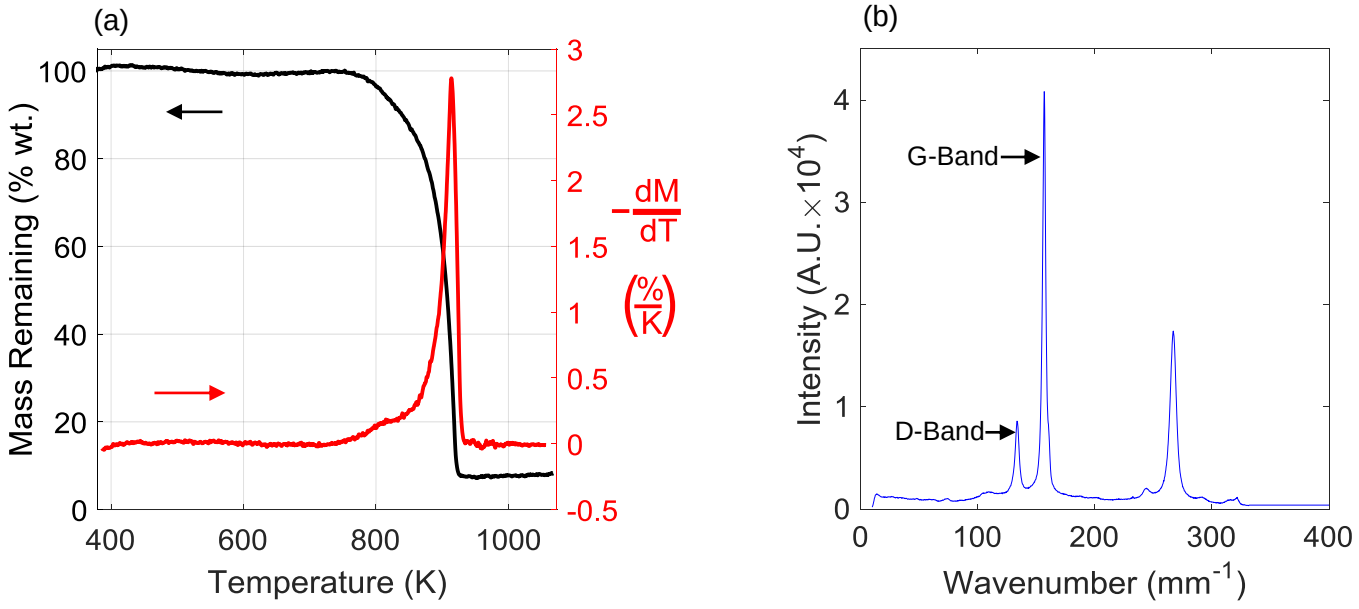

Figure A.1: (a) Thermogravimetric analysis of CNT mat in air, (b) Raman spectra of CNT mat.

References

[1] Michael F. L. De Volder, Sameh H. Tawfick, Ray H. Baughman, A. John Hart. “Carbon nanotubes: present and future commercial applications”. *Science*, 339, pp. 535-539 (2013).

[2] Bei Peng, Mark Locascio, Peter Zapol, Shuyou Li, Steven L. Mielke, George C. Schatz, Horacio D. Espinosa. “Measurements of near-ultimate strength for multiwalled carbon nanotubes and irradiation-induced crosslinking improvements”. *Nature Nanotechnology* 3, pp. 626-631 (2008).

[3] T. W. Ebbesen, H. J. Lezec, H. Hiura, J. W. Bennett, H. F. Ghaemi, T. Thio. “Electrical conductivity of individual carbon nanotubes”. *Nature,* 382, pp. 54-56 (1996).

[4] B. Q. Wei, R. Vajtai, P. M. Ajayan. “Reliability and current carrying capacity of carbon nanotubes”. *Applied Physics Letters,* 79, pp. 1172-1174 (2001).

[5] Eric Pop, David Mann, Qian Wang, Kenneth Goodson, Hongjie Dai. “Thermal conductance of an individual single-wall carbon nanotube above room temperature”. *Nano Letters,* 6, pp. 96-100 (2006).

[6] Ya-Li Li, Ian A. Kinloch, Alan H. Windle. “Direct spinning of carbon nanotube fibers from chemical vapor deposition synthesis”. *Science* 304, pp. 276-278 (2004).

[7] Belén Alemán, Victor Reguero, Bartolomé Mas, Juan J. Vilatela. “Strong carbon nanotube fibers by drawing inspiration from polymer fiber spinning”. *ACS Nano*, 9, pp. 7392-7398 (2015).

[8] Lorna J. Gibson, Michael F. Ashby. “*Cellular Solids”*. 2nd Edition, Cambridge Solid State Sciences, (1999).

[9] Natnael Behabtu, Colin C. Young, Dmitri E. Tsentalovich, Olga Kleinerman, Xuan Wang, Anson W. K. Ma, Amram Bengio, Ron F. ter Waarbeek, Jorrit J. de Jong, Ron E. Hoogerwerf, Steven B. Fairchild, John B. Ferguson, Benji Maruyama, Junichiro Kono, Yeshayahu Talmon, Yachin Cohen, Marcin J. Otto, Matteo Pasquali. "Strong, light, multifunctional fibers of carbon nanotubes with ultrahigh conductivity". Science 339, pp. 182-186, (2013).

[10] T. S. Gspann, F. R. Smail, A. H. Windle. “Spinning of carbon nanotube fibres using the floating catalyst high temperature route: purity issues and the critical role of sulphur”. *Faraday Discussions,* 173, pp. 47-65 (2014).

[11] Christian Hoecker, Fiona Smail, Martin Pick, Adam Boies. “The influence of carbon source and catalyst nanoparticles on CVD synthesis of CNT aerogel”. *Chemical Engineering Journal,* 314, pp. 388-395 (2017).

[12] Mukul Kumar, Yoshinori Ando. “Chemical vapor deposition of carbon nanotubes: a review on growth mechanism and mass production”. *Journal of Nanoscience and Nanotechnology,* 10, pp. 3739-3758 (2010).

[13] Shan Li, Xiaohua Zhang, Jingna Zhao, Fancheng Meng, Geng Xu, Zhenzhong Yong, Jingjing Jia, Zuoguang Zhang, Qingwen Li. “Enhancement of carbon nanotube fibres using different solvents and polymers”. *Composites Science and Technology,* 72, pp. 1402-1407 (2012).

[14] Horacio D. Espinosa, Tobin Filleter and Mohammed Naraghi. “Multiscale experimental mechanics of hierarchical carbon-based materials”. *Advanced Materials* 24, pp. 2805-2823, (2012).

[15] Min-Feng Yu, Bradley S. Files, Sivaram Arepalli, Rodney S. Ruoff. “Tensile loading of ropes of single wall carbon nanotubes and their mechanical properties”. *Physical Review Letters* 84, pp. 5552-5555, (2000).

[16] Jean-Paul Salvetat, G. Andrew D. Briggs, Jean-Marc Bonard, Revathi R. Bacsa, Andrezej J. Kulik. “Elastic and shear moduli of single-walled carbon nanotube ropes”. Physical Review Letters, 82, pp. 944-947 (1999).

[17] A. Kis, G. Csányi, J.-P. Salvetat, Thien-Nga Lee, E. Couteau, A. J. Kulik, W. Benoit, J. Brugger, L. Forró. “Reinforcement of single-walled carbon nanotube bundles by intertube bridging”. *Nature Materials*, 3, pp. 153-157 (2004).

[18] J. Z. Liu, Q.-S. Zheng, L.-F. Wang, Q. Jiang. “Mechanical properties of single-walled carbon nanotube bundles as bulk materials”. *Journal of Mechanics and Physics of Solids,* 53, pp. 123-142 (2005).

[19] A. Kis, K. Jensen, S. Aloni, W. Mickelson, A. Zettl. “Interlayer forces and ultralow sliding friction in multiwalled carbon nanotubes”. *Physical Review Letters*, 97, pp. 025501.1-4 (2006).

[20] Osamu Suekane, Atsuko Nagataki, Hideki Mori, Yoshikazu Nakayama. “Static friction force of carbon nanotube surfaces”. *Applied Physics Express*, 1, pp. 064001.1-3 (2008).

[21] Mohammad Naraghi, Graham H. Bratzel, Tobin Filleter, Zhi An, Xiaoding Wei, SonBinh T. Nguyen, Markus J. Buehler, Horacio D. Espinosa. “Atomistic investigation of load transfer between DWNT bundles “crosslinked” by PMMA oligomers”. *Advanced Functional Materials,* 23, pp. 1883-1892 (2012).
[22] Mohammad Naraghi, Tobin Filleter, Alexander Moravsky, Mark Locascio, Raouf O. Loutfy, Horacio D. Espinosa. “A multiscale study of high performance double-walled nanotube-polymer fibers”. *ACS Nano*, 4, pp. 6463-6476 (2010).
[23] Yuanyuan Shang, Ying Wang, Shuhiu Li, Chunfei Hua, Mingchu Zou, Anyuan Cao. “High-strength carbon nanotibers by twist-induced self-strengthening”. *Carbon*, 119, pp. 47-55, (2017).
[24] Rebekah Downes, Shaokai Wang, David Haldane, Andrew Moench, Richard Liang. “Strain-induced alignment mechanisms of carbon nanotube networks”. *Advanced Engineering Materials* 17, pp. 349-358 (2015).
[25] Fujun Xu, Baochun Wei, Wei Liu, Hongfei Zhu, Yongyi Zhang, Yiping Qiu. “In-plane mechanical properties of carbon nanotube films fabricated by floating catalyst chemical vapor decomposition”. *Journal of Materials Science,* 50, pp. 8166-8174 (2015).
[26] Agnieszka Lekawa-Raus, Krzysztof K. K. Koziol, Alan H. Windle. “Piezoresistive effect in carbon nanotube fibers”. *ACS Nano,* 8, pp. 11214-11224 (2014).
[27] “Standard Test Method for Tear-Propagation Resistance (Trouser Tear) of Plastic Film and Thin Sheeting by a Single-Tear Method”, ASTM D1938-14. ASTM International, West Conshohocken, PA, (2014).
[28] H. W. Greensmith, A. G. Thomas. “Rupture of rubber .3. determination of tear properties”. *Journal of Polymer Science* 18, pp. 189-200, (1955).
[29] “Standard Test Method for Peel Resistance of Adhesives (T-Peel Test)”, ASTM D1876-08. ASTM International, West Conshohocken, PA, (2015).
[30] V. S. Deshpande, M. F. Ashby, N. A. Fleck. “Foam topology: bending versus stretching dominated architectures”. *Acta Materialia*, 49, pp. 1035-1040, (2001).
[31] S. Timoshenko, J. N. Goodier. *Theory of Elasticity.* McGraw-Hill, (1970).
[32] J. C. Lasjaunias, K. Biljakovic, P. Monceau, J. L. Sauvajol. “Low-energy vibrational excitations in carbon nanotubes studied by heat capacity”. *Nanotechnology* 14, pp. 998-1003, (2003).
[33] Jeffrey T. Paci, Al’ona Furmanchuk, Horacio D. Espinosa, George C. Schatz. “Shear and friction between carbon nanotubes in bundles and yarns”. *Nano Letters*, 14, pp. 6138-3147 (2014).
[34] Xiaoding Wei, Mohammad Naraghi, Horacio D. Espinosa. “Optimal length scales emerging from shear load transfer in natural materials: application to carbon-based nanocomposite design”. *ACS Nano*, 6, pp. 2333-2344 (2012).
[35] A. Jorio, M. A. Pimenta, A. G. Souza Filho, R. Saito, G. Dresselhaus, M. S. Dresselhaus. “Characterizing carbon nanotube samples with resonance Raman scattering”. *New Journal of Physics* 5, pp. 139.1-17 (2003).
[36] A. C. Ferrari, J. Robertson. “Interpretation of Raman spectra of disordered and amorphous carbon”. *Physical Review B*, 61, 14095 (2000).

Supplementary Materials:

References for CNT-Based Material Property Chart Data

Review Papers:

[1] Agnieszka Lekawa-Raus, Jeff Patmore, Lukasz Kurzepa, John Bulmer, Krzysztof Koziol. “Electrical properties of carbon nanotube based fibers and their future use in electrical wiring”. Advanced Functional Materials 24 (2014), pp. 3661-3682.
[2] Stefania Nardecchia, Daniel Carriazo, M. Luisa Ferrer, María C. Gutiérrez and Francisco del Monte. “Three dimensional macroporous architectures and aerogels built of carbon nanotubes and/or graphene: synthesis and applications. “Chemical Society Reviews 42 (2013), pp. 794-830.
[3] Sherif Araby, Aidong Qiu, Ruoyu Wang, Zhiheng Zhao, Chun-Hui Wang, Jun Ma. “Aerogels based on carbon nanotube materials”. Journal of Materials Science 51 (2016), pp. 9157-9189.
[4] Eduard G. Rakov “Materials made of carbon nanotubes. The carbon nanotube forest”. Russian Chemical Reviews 82 (2013), pp. 538-566.
[5] Qing Cao, John A. Rogers. "Ultrathin films of single-walled carbon nanotubes for electronics and sensors: a review of fundamental and applied aspects". Advanced Materials 21 (2009), pp. 29-53.
[6] G. Gruner. "Carbon nanotube films for transparent and plastic electronics" Journal of Materials Chemistry 16 (2006), pp. 3533-3539.
[7] Hongwei Zhu, Bingqing Wei. "Assembly and applications of carbon nanotube thin films". Journal of Materials Science and Technology 24 (2008), pp. 447-456.
[8] Guanghui Xu, Qian Zhang, Weiping Zhou, Jiaqi Huang, Fei Wei. "The feasibiliy of producing MWCNT paper and strong MWCNT film from VACNT array". Applied Physics A 92 (2008), pp. 531-539.
[9] Jiangtao Di, Xin Wang, Yajuan Xing, Yongyi Zhang, Xiaohua Zhang, Weibang Liu, Qingwen Li, Yuntian T. Zhu. "Dry-processable carbon nanotubes for functional devices and composites". Small 10 (2014), pp. 4606-4625.
[10] Jiangtao Di, Xiaohua Zhang, Zhenzhong Yong, Yongyi Zhang, Da Li, Ru Li, Qingwen Li. "Carbon-nanotube fibers for wearable devices and smart textiles" Advanced Materials 28 (2016), pp. 10529-10538.
[11] Menghe Miao. "Yarn spun from carbon nanotube forests: Production, structure, properties and applications". Particuology 11 (2013) pp. 378-393.
[12] Natnael Behabtu, Micah J. Green, Matteo Pasquali. "Carbon nanotube-based neat fibers" Nanotoday 3 (2008), pp. 24-34.
[13] Tsu-Wei Chou, Limin Gao, Erik T. Thostenson, Zuoguang Zhang, Joon-Hyung Byun. "An assessment of the science and technology of carbon nanotube-based fibers and composites". Composites Science & Technology 70 (2010) pp. 1-19.
[14] Kaili Jiang, Qunqing Li, Shoushan Fan. "Nanotechnology: Spinning continuous carbon nanotube yarns". Nature 419 (2002), pp. 801.
[15] Kaili Jiang, Jiaping Wang, Qunqing Li, Liang Liu, Changhong Liu, Shoushan Fan. "Superaligned carbon nanotube arrays, films, and yarns: a road to applications". Advanced materials 23 (2011), pp. 1154-1161.
[16] Junbeom Park, Kun-Hong Lee. "Carbon Nanotube Yarns". Korean Journal of Chemical Engineering 29 (2012) pp. 277-287.

Yarns spun from arrays/forests:

[1] Ali E. Aliev, Csaba Guthy, Mei Zhang, Shaoli Fang, Anvar A. Zakhidov, John E. Fischer, Ray H. Baughman. "Thermal transport in MWNT sheets and yarns" Carbon 45 (2007), pp. 2880-2888.
[2] Ken R. Atkinson, Stephen C. Hawkins, Chi Huynh, Chris Skourtis, Jane Dai, Mei Zhang, Shaoli Fang, Anvar A. Zakhidov, Sergey B. Lee, Ali E. Aliev, Christopher D. Williams, Ray H. Baughman. "Multifunctional carbon nanotube yarns and transparent sheets: Fabrication, properties and applications". Physica B, 394 (2007), 339-343.
[3] Alexander E. Bogdanovich, Philip D. Bradford. "Carbon nanotube yarn and 3D braid composites: part I: tensile testing and mechanical properties analysis". Composites Part. A, 41 (2010) pp. 230-237.

[4] Fei Deng, Weibang Lu, Haibo Zhao, Yuntian Zhu, Byung-Sun Kim, Tsu-Wei Chou. "The properties of dry-spun carbon nanotube fibers and their interfacial shear strength in an epoxy composite". Carbon 49 (2011), pp. 1752-1757.
[5] Shaoli Fang, Mei Zhang, Anvar A. Zakhidov, Ray H. Baughman. "Structure and process-dependent properties of solid-state spun carbon nanotube yarns". Journal of Physics and Condensed Matter 22 (2010), pp. 334221.
[6] Menghe Miao. "Electrical conductivity of pure carbon nanotube yarns". Carbon 49 (2011) pp. 3755-3761.
[7] Menghe Miao, Stephen C. Hawkins, Jackie Y. Cai, Thomas R. Gengenbach, Robert Knott, Chi P. Huynh. "Effect of gamma-irradiation on the mechanical properties of carbon nanotube yarns". Carbon 49 (2011) pp. 4940-4947.
[8] Xiefei Zhang, Qingwen Li, Yi Tu, Yuan Li, James Y. Coulter, Lianxi Zheng, Yonghao Zhao, Qianxi Jia, Dean E. Peterson, Yuntian Zhu. "Strong carbon-nanotube fibers spun from long carbon-nanotube arrays". Small 3 (2007), pp. 244-248.
[9] Xiefei Zhang, Qingwen Li, Terry G. Holesinger, Paul N. Arendt, Jianyu Huang, P. Douglas Kirven, Timothy G. Clapp, Raymond F. DePaula, Xiazhou Liao, Yonghao Zhao, Lianxi Zheng, Dean E. Peterson, Yuntian Zhu. "Ultrastrong, stiff and lightweight carbon nanotube fibres". Advanced materials 19 (2007), pp. 4198-4201.
[10] Shanju Zhang, Lingbo Zhu, Marilyn L. Minus, Han Gi Chae, Sudhakar Jagannathan, Ching-Ping Wong, Janusz Kowalik, Luke B. Robertson, Satish Kumar. "Solid-state spun fibers and yarns from 1-mm long carbon nanotube forests synthesized by water-assisted chemical vapor deposition". Journal of Materials Science 43 (2008), pp. 4356-4362.
[11] Kai Liu, Yinghui Sun, Ruifeng Zhou, Hanyu Zhu, Jiaping Wang, Liang Liu, Shoushan Fan, Kaili Jiang. "Carbon nanotube yarns with high tensile strength made by a twisting and shrinking method". Nanotechnology, 21(2010), 045708.
[12] Mei Zhang, Ken R. Atkinson, Ray H. Baughman. "Multifunctional carbon nanotube yarns by downsizing an ancient technology". Science 306 (2004), pp. 1358-1361.
[13] Jiangtao Di, Shaoli Fang, Francisco A. Moura, Douglas S. Galvão, Julia Bykova, Ali Aliev, Mônica Jung de Andrade, Xavier Lepró, Na Li, Carter Haines, Raquel Ovalle-Robles, Dong Qian, Ray H. Baughman. "Strong, twist-stable carbon nanotube yarns and muscles by tension annealing at extreme temperatures". Advanced Materials 28 (2016), pp. 6598-6605.
[14] Jandro L. Abot, Tareq Alosh, Kalayu Belay. "Strain dependence of electrical resistance in carbon nanotube yarns". Carbon 70 (2014) pp. 95-102.
[15] Yoshinobu Shimamura, Kahori Oshima, Keiichiro Tohgo, Tomoyuki Fujii, Keiichi Shirasu, Go Yamamoto, Toshiyuki Hashida, Ken Goto, Toshio Ogasawara, Kimiyoshi Naito, Takayuki Nakano, Yoku Inoue. "Tensile mechanical properties of carbon nanotube/epoxy composite fabricated by pultrusion of carbon nanotube spun yarn preform". Composites: Part A 62 (2014), pp. 32-38.
[16] Jackie Y. Cai, Jie Min, Jill McDonnell, Jeffrey S. Church, Christopher D. Easton, William Humphries, Stuart Lucas, Andrea L. Woodhead. "An improved method for functionalisation of carbon nanotube spun yarns with aryldiazonium compounds". Carbon 50 (2012), pp. 4655-4662.
[17] Adrian Ghemes, Yoshitaka Minami, Junichi Muramatsu, Morihiro Okada, Hidenori Mimura, Yoku Inoue. "Fabrication and mechanical properties of carbon nanotube yarns spun from ultra-long multi-walled carbon nanotube arrays". Carbon 50 (2012), pp. 4579-4587.
[18] Mei Zu, Qingwen Li, Yuntian Zhu, Yong Zhu, Guojian Wang, Joon-Hyung Byun, Tsu-Wei Chou. "Stress relaxation in carbon nanotube-based fibers for load-bearing applications" Carbon 52 (2013) pp. 347-355.

Mats drawn from arrays/forests:

[1] Mei Zhang, Shaoli Fang, Anvar A. Zakhidov, Sergey B. Lee, Ali E. Aliev, Christopher D. Williams, Ken R. Atkinson, Ray H. Baughman. "Strong, transparent, multifunctional, carbon nanotube sheets". Science 309 (2005), pp. 1215-1219.
[2] Ken R. Atkinson, Stephen C. Hawkins, Chi Huynh, Chris Skourtis, Jane Dai, Mei Zhang, Shaoli Fang, Anvar A. Zakhidov, Sergey B. Lee, Ali E. Aliev, Christopher D. Williams, Ray H. Baughman. "Multifunctional carbon nanotube yarns and transparent sheets: fabrication, properties and applications". Physica B: Condensed Mater 394 (2007), pp. 339-343.

[3] Ali E. Aliev, Csaba Guthy, Mei Zhang, Shaoli Fang, Anvar A. Zakhidov, John E. Fischer, Ray H. Baughman. "Thermal transport in MWCNT sheets and yarns" Carbon 45 (2007), pp. 2880-2888.
[4] Liwen Zhang, Xin Wang, Weizong Xu, Yongyi Zhang, Qingwen Li, Philip D. Bradford, Yuntian Zhu. "Strong and conductive dry carbon nanotube films by microcombing" Small 11 (2015), pp. 3830-3836.
[5] Ding Wang, Pengcheng Song, Canghong Liu, Wei Wu, Shoushan Fan. "Highly oriented carbon nanotube papers made of aligned carbon nanotubes" Nanotechnology 19 (2008), 075609.
[6] Yoku Inoue, Yusuke Suzuki, Yoshitaka Minami, Junichi Muramatsu, Yoshinobu Shimamura, Katsunori Suzuki, Adrian Ghemes, Morihiro Okada, Shingo Sabakibara, Hidenori Mimura, Kimiyoshi Naito. "Anisotropic carbon nanotube papers fabricated from multiwalled carbon nanotube webs". Carbon 49 (2011), pp. 2437-2443.
[7] Jiangtao Di, Dongmei Hu, Hongyuan Chen, Zhenzhong Yong, Minghai Chen, Zhihai Feng, Yuntian Zhu, Qingwen Li. "Ultrasrong, foldable, and highly conductive carbon nanotube film". ACS Nano 6 (2012), pp. 5457-5464.
[8] Yanjie Wang, Min Li, Yizhuo Gu, Xiaohua Zhang, Shaokai Wang, Qingwen Li, Zuoguang Zhang. "Tuning carbon nanotube assembly for flexible, strong and conductive films". Nanoscale 7 (2015), pp. 3060-3066.

Buckypapers:

[1] Chunming Niu, Enid K. Sichel, Robert Hoch, David Moy, Howard Tennent. "High power electrochemical capacitors based on carbon nanotube electrodes" Applied Physics Letters 70 (1997), pp. 1480-1482.
[2] Ray H. Baughman, Changxing Cui, Anvar A. Zakhidov, Zafar Iqbal, Joseph N. Barisci, Geoff M. Spinks, Gordon G. Wallace, Alberto Mazzoldi, Danilo De Rossi, Andrew G. Rinzler, Oliver Jaschinski, Siegmar Roth, Miklos Kertesz. "Carbon Nanotube Actuators". Science 284 (1999), pp. 1340-1344.
[3] Shiren Wang, Zhiyong Liang, Ben Wang, Chuck Zhang. "High-strength and multifunctional macroscopic fabric of single-walled carbon nanotubes". Advanced Materials 19 (2007), pp. 1257-1261.
[4] T. V. Sreekumar, Tao Liu, Satish Kumar, Lars M. Ericson, Robert H. Hauge, Richard E. Smalley "Single-wall carbon nanotube films". Chemistry of Materials 15 (2003), pp. 175-178.
[5] Ding Wang, Pengcheng Song, Canghong Liu, Wei Wu, Shoushan Fan. "Highly oriented carbon nanotube papers made of aligned carbon nanotubes" Nanotechnology 19 (2008), 075609.
[6] A. D. Bozhko, D. E. Sklovsky, V. A. Nalimova, A. G. Rinzler, R. E. Smalley, J. E. Fischer. "Resistance vs. pressure of single-wall carbon nanotubes" Applied Physics A 67 (1998), pp. 75-77.
[7] Philip G. Whitten, Adrian A. Gestos, Geoffrey M. Spinks, Kerry J. Gilmore, Gordon G. Wallace. "Free standing carbon nanotube composite bio-electrodes" Journal of Biomedical Materials Research Part B: Applied Biomaterials 82B (2007), pp. 37-43.
[8] Sharali Malik, Harald Rösner, Frank Hennrich, Artur Böttcher, Manfred M. Kappes, Tilmann beck, Markus Auhorn. "Failure mechanism of free standing single-walled carbon nanotube thin films under tensile load" Physical Chemistry Chemical Physics 6 (2004), pp. 3540-3544.
[9] I-Wen Peter Chen, Richard Liang, Haibo Zhao, Ben Wang, Chuck Zhang. "Highly conductive carbon nanotube buckypapers with improved doping stability via conjugational cross-linking". Nanotechnology 22 (2011), 485708.
[10] Wen-Tai Hong, Nyan-Hwa Tai. "Investigations on the thermal conductivity of composites reinforced with carbon nanotubes" Diamond and Related materials 17 (2008), pp. 1577-1581.
[11] Hongyuan Chen, Minghai Chen, Jiangtao Di, Geng Xu, Hongbo Li, Qingwen Li. "Architecting three-dimensional networks in carbon nanotube buckypapers for thermal interface materials". Journal of Physical Chemistry C 116 (2012), pp. 3903-3909.
[12] J. E. Fischer, W. Zhou, J. Vavro, M. C. Llaguno, C. Guthy, R. Haggenmueller, M. J. Casavant, D. E. Walters, R. E. Smalley. "Magnetically aligned single wall carbon nanotube films: preferred orientation and anisotropic transport properties" Journal of Applied Physics 93 (2003), pp. 2157-2163.
[13] Michael B. Jukubinek, Benham Ashrafi, Jingwen Guan, Michael B. Johnson, Mary Anne White, Benoit Simard. "3D chemically cross-linked single-walled carbon nanotube buckypapers". RSC Advances 4 (2014), pp. 57564-57573.

Fibres spun from solutions:

[1] Lars M. Ericson, Hua Fan, Haiqing Peng, Virginia A. Davis, Wei Zhou, Joseph Sulpizio, Yuhuang Wang, Richard Brooker, Juraj Vavro, Csaba Guthy, A. Nicholas G. Parra-Vasquez, Myung Jong Kim, Sivarajan Ramesh, Rajesh K. Saini, Carter Kittrell, Gerry Lavin, Howard Schmidt, W. Wade Adams, W. E. Billups, Matteo Pasquali, Wen-Fang Hwang, Robert H. Hauge, John E. Fischer, Richard E. Smalley. "Macroscopic, neat, single-walled carbon nanotube fibers". Science 305 (2004), pp. 1447-1450.
[2] Chengmin Jiang, Avishek Saha, Colin C. Young, Daniel Paul Hashim, Carolyn E. Ramirez, Pulickel M. Ajayan, Matteo Pasquali, Angel A. Marti. "Macroscopic nanotube fibers spun from single-walled carbon nanotube polyelectrolytes". ACS Nano 8 (2014), pp. 9107-9112.
[3] L. Piraux, F. Abreu Araujo, T. N. Biu. "Two-dimensional quantum transport in highly conductive carbon nanotube fibers". Physical Review B 92 (2015), 085428.
[4] Natnael Behabtu, Colin C. Young, Dmitri E. Tsentalovich, Olga Kleinerman, Xuan Wang, Anson W. K. Ma, Amram Bengio, Ron F. ter Waarbeek, Jorrit J. de Jong, Ron E. Hoogerwerf, Steven B. Fairchild, John B. Ferguson, Benji Maruyama, Junichiro Kono, Yeshayahu Talmon, Yachin Cohen, Marcin J. Otto, Matteo Pasquali. "Strong, light, multifunctional fibers of carbon nanotubes with ultrahigh conductivity". Science 339 (2013), pp. 182-186.
[5] Francesca Mirri, Nathan D. Orloff, Aaron M. Forster, Rana Ashkar, Robert J. Headrick, E. Amram Bengio, Christian J. Long, April Choi, Yimin Luo, Angela R. Hight Walker, Paul Butler, Kalman B. Migler, Matteo Pasquali. "Lightweight, flexible, high-performance carbon nanotube cables made by scalable flow coating". Applied Materials & Interfaces 8 (2016), pp. 4903-4910.
[6] Don Shiffler, Steve Fairchild, Wilkin Tang, Benji Maruyama, Ken Golby, Matthel LaCour, Matteo Pasquali, Nathaniel Lockwood. "Demonstration of an acid-spun single-walled nanotube fiber cathode". IEEE Transactions on Plasma Science 40 (2012), pp. 1871-1877.
[7] S. B. Fairchild, J. Boeckl, T. C. Back, J. B. Ferguson, H. Koerner, P. T. Murray, B. Maruyama, M. A. Lange, M. M. Cahay, N. Behabtu, C. C. Young, M. Pasquali, N. P. Lockwood, K. L. Averett, G. Grun, D. E. Tsentalovich. "Morphology dependent field emission of acid-spun carbon nanotube fibers". Nanotechnology 26 (2015) 105706.
[8] Xuan Wang, Natnael Behabtu, Colin C. Young, Dmitri E. Tsentalovich, Matteo Pasquali, Junichiro Kono. "High-ampacity power cables of tightly-packed and aligned carbon nanotubes" Advanced Functional Materials 24 (2014), pp. 3241-3249.

Direct-spun mats:

[1] Jian-Min Feng, Rui Wang, Ya-Li Li, Xiao-Hua Zhong, Lan Cui, Qian-Jin Guo, Feng Hou. "One-step fabrication of high quality double-walled carbon nanotube thin films by a chemical vapor deposition process". Carbon 48 (2010), pp. 3817-3824.
[2] I. Stuart Fraser, Marcelo S. Motta, Ron K. Schmidt, Alan H. Windle. "Continuous production of flexible carbon nanotube-based transparent conductive films". Science and Technology of Advanced Materials 11 (2010), 045004.
[3] Dawid Janas, Krzysztof K. Kozio. "Rapid electrothermal response of high-temperature carbon nanotube film heaters". Carbon 59 (2013), pp. 457-463.
[4] Jae-Woo Kim, Emilie J. Siochi, Jennifer Carpena-Nunez, Kristopher E. Wise, John W. Connell, Yi Lin, Russell A. Wincheski. "Polyaniline/carbon nanotube sheet nanocomposites: fabrication and characterization". ACS Applied Materials & Interfaces 5 (2013), pp. 8597-8606.
[5] Jae-Woo Kim, Godfrey Sauti, Emilie J. Siochi, Joseph G. Smith, Russell A. Wincheski, Roberto J. Cano, John W. Connell, Kristopher E. Wise. "Toward high performance thermoset/carbon nanotube sheet nanocomposites via resistive heating assisted infiltration and cure". Applied Materials & Interfaces 6 (2014), pp. 18832-18843.
[6] Peng Liu, Thang Q. Tran, Zeng Fan, Hai M. Duong. "Formation mechanisms and morphological effects on multi-properties of carbon nanotube fibers and their polyimide aerogel-coated composites". Composites Science and Technology 117 (2015), pp. 114-120.
[7] Fengmei Guo, Can Li, Jianquan Wei, Ruiqiao Xu, Zelin Zhang, Kunlin Wang, Dehai Wu. "Fabrication of highly conductive carbon nanotube fibers for electrical application". Materials Research Express 2 (2015), 095604.

[8] Fujun Xu, Baochun Wei, Wei Liu, Hongfei Zhu, Yongyi Zhang, Yiping Qiu."In-plane mechanical properties of carbon nanotube films fabricated by floating catalyst chemical vapour decomposition". Journal of Materials Science 50 (2015), pp. 8166-8174.
[9] Min Li, Zhenzhen Wang, Qianli Liu, Shaokai Wang, Yizhuo Gu, Yanxia Li, Zuoguang Zhang. "Carbon nanotube film/epoxy composites with high strength and toughness". Polymer Composites 38 (2017), pp. 588-596.
[10] Joseph Severino, Jenn-Ming Yang, Larry Carlson, Robert Hicks. "Progression of alignment in stretched CNT sheets determined by wide angle X-ray scattering". Carbon 100 (2016), pp. 309-317.
[11] Jiali Yu, Weibang Lu, Shaopeng Pei, Ke Gong, Liyun Wang, Linghui Meng, Yudong Huang, Joseph P. Smith, Karl S. Booksh, Qingwen Li, Joon-Hyung Byun, Youngseok Oh, Yushan Yan, Tsu-Wei Chou. "Omnidirectionally stretchable high-performance supercapacitor based on isotropic buckled carbon nanotube films". ACS Nano 10 (2016), pp. 5204-5211.
[12] Heath E. Misak, James L. Rutledge, Eric D. Swenson, Shankar Mall. "Thermal transport properties of dry spun carbon nanotube sheets". Journal of Nanomaterials (2016), 9174085.
[13] Peng Liu, Zeng Fan, Anastasiia Mikhalchan, Thang Q. Tran, Daniel Jewell, Hai M. Duong, Amy M. Marconnet."Continuous carbon nanotube-based fibers and films for applications requiring enhanced heat dissipation". Applied Materials & Interfaces 8 (2016), pp. 17461-17471
[14] Wenjun Ma, Li Song, Rong Yang, Taihua Zhang, Yuanchun Zhao, Lianfeng Sun, Yan Ren, Dongfang Liu, Lifeng Liu, Jun Shen, Zhengxing Zhang, Yanjuan Xiang, Weiya Zhou, SiShen Xie. "Directly synthesized strong, highly conducting, transparent single-walled carbon nanotube films". Nano Letters 7 (2007), pp. 2307-2311.
[15] Jacob W. Singleton, Heath E. Misak, Shankar Mall. "Relationships between tensile behaviour, physical parameters and manufacturing parameters of carbon nanotube sheet". Materials & Design 116 (2017), pp. 199-206.
[16] Qianli Liu, Min Li, Yizhuo Gu, Yongyi Zhang, Shaokai Wang, Qingwen Li, Zuoguang Zhang. "Highly aligned dense carbon nanotube sheets induced by multiple stretching and pressing". Nanoscale 6 (2014), pp. 4338-4344.
[17] Jinquan Wei, Hongwei Zhu, Yanhui Li, Bin Chen, Yi Jia, Kunlin Wang, Zhicheng Wang, Wenjin Liu, Jianbin Luo, Mingxin Zheng, Dehai Wu, Yanqiu Zhu, Bingqing Wei. "Ultrathin single-layered membranes from double-walled carbon nanotubes" Advanced Materials 18 (2006), pp. 1695-1700.
[18] Wenjun Ma, Luqi Liu, Rong Yang, Taihua Zhang, Zhong Zhang, Li Song, Yan Ren, Jun Shen, Zhiqiang Niu, Weiya Zhou, Sishen Xie. "Monitoring a micromechanical process in macroscale carbon nanotube films and fibers". Advanced Materials 21 (2009), pp. 603-608.
[19] Jack Alvarenga, Paul R. Jarosz, Chris M. Schauerman, Brian T. Moses, Brian J. Landi, Cory D. Cress, Ryne P. Raffaelle. "High conductivity carbon nanotube wires from radial densification and ionic doping". Applied Physics Letters 97 (2010), 182106.

Direct-spun fibres & Aerogels from the Gas Phase:

[1] J. N. Wang, X. G. Luo, T. Wu, Y. Chen. "High-strength carbon nanotube fibre-like ribbon with high ductility and high electrical conductivity". Nature Communications, 5, (2014), 3848.
[2] Marcelo Motta, Ya-Li Li, Ian Kinloch, Alan Windle. "Mechanical properties of continuously spun fibers of carbon nanotubes". Nano Letters 5 (2005), pp. 1529-1533.
[3] Krzysztof Koziol, Juan Vilatela, Anna Moisala, Marcelo Motta, Philip Cunniff, Michael Sennett, Alan Windle. "High-performance carbon nanotube fiber". Science 318 (2007), pp. 1892-1895.
[4] Kelly L. Stano, Krzysztof Koziol, Martin Pick, Marcelo S. Motta, Anna Moisala, Juan J. Vilatela, Stuart Frasier, Alan H. Windle. "Direct spinning of carbon nanotube fibres from liquid feedstock". International Journal of Material Forming, 1 (2008), pp. 59-62.
[5] J. Chaffee, D. Lashmore, D. Lewis, J. Mann, M. Schauer, B. White. "Direct synthesis of CNT yarns and sheets". NSTI-Nanotech, (2008), pp. 118-121.
[6] Richard J. Davies, Christian Riekel, Krzysztof K. Koziol, Juan J. Vilatela, Alan H. Windle. "Structural studies on carbon nanotube fibres by synchrotron radiation microdiffraction and microfluorescence". Journal of Applied Crystallography 42 (2009), pp. 1122-1128.
[7] R. J. Mora, J. J. Vilatela, A. H. Windle. "Properties of composites of carbon nanotube fibres". Composites Science and Technology 69 (2009), pp. 1558-1563.
[8] Xiao-Hua Zhong, Ya-Li Li, Ya-Kun Liu, Xiao-Hua Qiao, Yan Feng, Ji Liang, Jun Jin, Lu Zhu, Feng Hou, Jin-You Li. "Continuous multilayered carbon nanotube yarns". Advanced Materials 22 (2010), pp. 692-696.

[9] Mark W. Schauer, David S. Lashmore, Diana J. Lewis, Benjamin M. Lewis, Erik C. Towle. "Strength and electrical conductivity of carbon nanotube yarns". Material Research Society Syposium Proceedings, 1258 (2010).
[10] Frances A. Hill. "Mechanical Energy Storage in Carbon Nanotube Springs". PhD Thesis, MIT, (2011)
[11] Qiu Li, Yi-Lan Kang, Wei Qiu, Ya-Li Li, Gan-Yun Huang, Jian-Gang Guo, Wei-Lin Deng, Xiao-Hua Zhong. "Deformation mechanisms of carbon nanotube fibres under tensile loading by in situ Raman spectroscopy analysis". Nanotechnology 22 (2011), 225704.
[12] Amanda S. Wu, Xu Nie, Matthew C. Hudspeth, Weinong W. Chen, Tsu-Wei Chou, David S. Lashmore, Mark W. Schauer, Erick Tolle, Jeff Rioux. "Strain rate-dependent tensile properties and dynamic electromechanical response of carbon nanotube fibers". Carbon 50 (2011), pp. 3876-3881.
[13] Amanda S. Wu, Tsu-Wei Chou, John W. Gillespie, Jr., David Lashmore, Jeff Rioux."Electromechanical response and failure behaviour of aerogel-spun carbon nanotube fibres under tensile loading". Journal of Materials Chemistry 22 (2012), pp. 6792-6798.
[14] Xiao-Hua Zhong, Ya-Li Li, Jian-Min Feng, Yan-Ru Kang, Shuai-Shuai Han. "Fabrication of a multifunctional carbon nanotube "cotton" yarn by the direct chemical vapour deposition spinning process". Nanoscale 4 (2012), pp. 5614-5618.
[15] Juan J. Vilatela, Alan H. Windle. "A multifunctional yarn made of carbon nanotubes". Journal of Engineered Fibers and Fabrics, Special Issue, (2012), pp. 23-28.
[16] V. Sabelkin, H. E. Misak, S. Mall, R. Asmatulu, P. E. Kladitis. "Tensile loading behaviour of carbon nanotube wires". Carbon 50 (2012), pp. 2530-2538.
[17] Yong-Mun Choi, Hungo Choo, Hyeonuk Yeo, Nam-Ho You, Dong Su Lee, Bon-Cheol Ku, Hwan Chul Kim, Pill-Hoon Bong, YoungJin Jeong, Munju Goh. "Chemical method for improving both the electrical conductivity and mechanical properties of carbon nanotube yarn via intramolecular cross-dehydrogenative coupling". ACS Applied Materials & Interfaces 5 (2013), pp. 7726-7730.
[18] H. E. Misak, V. Sabelkin, S. Mall, P. E. Kladitis. "Thermal fatigue and hypothermal atomic oxygen exposure behaviour of carbon nanotube wires". Carbon 57 (2013), pp. 42-49.
[19] Frances A. Hill, Timothy F. Havel, David Lashmore, Mark Schauer, Carol Livermore. "Storing energy and powering small systems with mechanical springs made of carbon nanotube yarn". Energy 76 (2014), pp. 318-325.
[20] A. Abu Obaid, D. Heider, J. W. Gillespie Jr. "Investigation of electro-mechanical behaviour of carbon nanotube yarns during tensile loading". Carbon 93 (2015), pp. 731-741.
[21] Fengmei Guo, Can Li, Jianquan Wei, Ruiqiao Xu, Zelin Zhang, Kunlin Wang, Dehai Wu. "Fabrication of highly conductive carbon nanotube fibers for electrical application" Materials Research Express 2 (2015), 095604.
[22] H. E. Misak, S. Mall. "Electrical conductivity, strength and microstructure of carbon nanotube multi-yarns". Materials and Design 75 (2015), pp. 76-84.
[23] H. E. Misak, S. Mall. "Time-dependent electrical properties of carbon nanotube yarns". New Carbon Materials 30 (2015), pp. 207-213.
[24] Thang Q. Tran, Zeng Fan, Anastasiia Mikhalchan, Peng Liu, Hai M. Duong. "Post-treatments for multifunctional property enhancement of carbon nanotube fibers from the floating catalyst method". Applied Materials & Interfaces 8 (2016), pp. 7948-7956.
[25] Peng Liu, Zeng Fan, Anastasiia Mikhalchan, Thang Q. Tran, Daniel Jewell, Hai M. Duong, Amy M. Marconnet."Continuous carbon nanotube-based fibers and films for applications requiring enhanced heat dissipation". Applied Materials & Interfaces 8 (2016), pp. 17461-17471
[26] Yanan Yue, Kang Liu, Man Li, Xuejiao Hu. "Thermal manipulation of carbon nanotube fiber by mechanical stretching". Carbon 77 (2014), pp. 973-979.
[27] Anyuan Cao, Pamela L. Dickrell, W. Gregory Sawyer, Mehrdad N. Ghasemi-Nejhad, Pulickel M. Ajayan. “Super-compressible fomalike carbon nanotube films”. Science 310 (2005), pp. 1307-1310.

CNT Foams:

[1] Xuchan Gui, Jinquan Wei, Kunlin Wang, Anyuan Cao, Hongwei Zhu, Yi Jia, Qinke Shu, Dehai Wu. “Carbon nanotube sponges”. Advanced materials 22 (2010), pp. 617-621.
[2] Xuchun Gui, Anyuan Cao, Jinquan Wei, Hongbian Li, Yi Jia, Lili Fan, Kunlin Wang, Hongwei Zhu, Dehai Wu. “Soft, highly conductive nanotube sponges and composites with controlled compressibility”. ACS Nano 4 (2010), pp. 2320-2326.
[3] Ryan R. Kohlmeyer, Maika Lor, Jian Deng, Haiying Liu, Jian Chen. “Preparation of stable carbon nanotube aerogels with high electrical conductivity and porosity”. Carbon 49 (2011), pp. 2352-2361.

[4] Marcus A. Worsley, Joe H. Satcher Jr, Theodore F. Baumann. “Synthesis and characterization of monolithic carbon aerogel nanocomposites containing double-walled carbon nanotubes”. Langmuir 24 (2008), pp. 9763-9766.
[5] Marcus A. Worsley, Sergei O. Kucheyev, Joshua D. Kuntz, Tammy Y. Olson, T. Yong-Jin Han, Alex V. Hamza, Joe H. Satcher, Jr., Theodore F. Baumann. “Carbon scaffolds for stiff and highly conductive monolithic oxide-carbon nanotube scaffolds”. Chemistry of Materials 23 (2011), pp. 3504-3061.
[6] Marcus A. Worsley, Sergei O. Kucheyev, Joe H. Satcher, Jr., Alex V. Hamza, Theodore F. Baumann. “Mechanically robust and electrically conductive carbon nanotube foams”. Applied Physics Letters 94 (2009), 073115.
[7] Marcus A. Worsley, Peter J. Pauzauskie, Sergei O. Kucheyev, Joseph M. Zaug, Alex V. Hamza, Joe H. Satcher Jr., Theodore F. Baumann. “Properties of single-walled carbon nanotube-based aerogels as a function of nanotube loading”. Acta Materialia 57 (2009), pp. 5131-5136.
[8] Zhuyin Sui, Qinghan Meng, Xuetong Zhang, Rui Ma, Bing Cao. “Green synthesis of carbon nanotube-graphene hybrid aerogels and their use as versatile agents for water purification”. Journal of Materials Chemistry 22 (2012), pp. 8767-8771.
[9] Jianhua Zou, Jianhua Liu, Ajay Singh Karakoti, Amit Kumar, Daeha Joung, Qiang Li, Saiful I. Khondaker, Sudipta Seal, Lei Zhai. “Ultralight multiwalled carbon nanotube aerogel”. ACS Nano 4 (2010), pp. 7293-7302.
[10] Xuetong Zhang, Jiren Liu, Bin Xu, Yuefeng Su, Yunjun Luo. “Ultralight conducting polymer/carbon nanotube composite aerogels”. Carbon 49 (2011), pp. 1884-1893.
[11] Yufeng Luo, Shu Luo, Hengcai Wu, Mengya Li, Ke Wang, Lingjia Yan, Kaili Jiang, Qunqing Li, Shoushan Fan, Jiaping Wang. "Self-expansion construction of ultralight carbon nanotube aerogels with a 3D and hierarchical cellular structure". Small, 13 (2017), 1700966.
[12] Shaghayegh Faraji, Kelly L. Stano, Ozkan Yildiz, Ang Li, Yuntian Zhu, Philip D. Bradford. "Ultralight anisotropic foams from layered aligned carbon nanotube sheets". Nanoscale 7 (2015), 17038.

Voigt Bounds:

Voigt Bounds for electrical and thermal conductivity material property charts are based on data from:

[1] T. W. Ebbesen, H. J. Lezec, H. Hiura, J. W. Bennett, H. F. Ghaemi, T. Thio. “Electrical conductivity of individual carbon nanotubes”. *Nature,* 382, pp. 54-56 (1996).
[2] Eric Pop, David Mann, Qian Wang, Kenneth Goodson, Hongjie Dai. “Thermal conductance of an individual single-wall carbon nanotube above room temperature”. *Nano Letters,* 6, pp. 96-100 (2006).
[3] C. Y. Ho, R. W. Powell, P. E. Liley. “Thermal conductivity of the elements: a comprehensive review”. *Journal of Physical and Chemical Reference Data*, Vol. 3, Supplement No. 1, (1974).